**NKFI Grant** NN-118089

**Title:** *Epigenetic regulation of ABA signal transduction: function of ZFP3 zinc finger factor in regulation of chromatin remodeling.*

**Principal Investigator:** dr. László Szabados

**Final report.**

In this report we are giving an overview of the research activities which were performed within the frame of the research grant. We give a brief description of the experiments, the results, and describe the efforts we made to pursue our goals.

**Attempts to identify ZFP3 interacting proteins.**

Preliminary results suggested, that ZFP3 can interact with chromatin remodelling factors. Therefore we decided to test possible interaction of ZFP3 with members of the chromatin remodelling complexes in several experimental systems: yeast two hybrid (Y2H), Bimolecular fluorescence complementation assay (BiFC) and Immunoprecipitation coupled with mass spectrometry.

*Yeast two hybrid tests.*

In order to perform pairwise Y2H assays, ZFP3 and components of the SWI/SNF complex (BRM, SWI3A, SWI3B, SWI3C, SWI3D) were cloned into Y2H vectors pGADT7 (prey) or pGBKT7 (bait) and their pairwise interaction was tested in yeast strains PJ69-4a or Y190. Growth of yeast colonies in selective media, in the presence of 3AT was tested in different combinations. Using PJ69-4a strain, ZFP3 in both vectors did not show self activation. BRM showed strong self activation in pGBKT7, and weaker but definite self activation in pGADT7. Combination of ZFP3 with BRM did not enhanced growth or it was slightly superior on selective medium than with the BRM and ZFP3 factors alone (Figure 1). Using other strains such as AH109 or Y190 for Y2H assays, gave similar results. When interaction of ZFP3 with other subunits of the complex was tested (SWI3A, SWI3B, SWI3C, SWI3D), negative results were obtained (not shown). These results could not confirm definite interaction of ZFP3 with subunits of the SWI/SNF complex: BRM, neither with SWI3A, SWI3B, SWI3C, SWI3D. Due to the nature of the Y2H system, interactions had to be tested with independent methods.

*BiFC assays*

Bimolecular fluorescence complementation assay (BiFC) is suitable for detecting the interaction of two proteins in living plant cells. To test interaction of ZFP3 and Brahma (BRM), both proteins were cloned into SPYNE and SPYCE vectors in N and C terminal fusions with truncated YFP marker. Agrobacterium-mediated transient expression was made with Arabidopsis cell suspensions and Nicotianve benthamiana leaves.

The following combinations were used in each experiment:
1. BRM_N
2. BRM_C
3. ZFP3_N

4. ZFP3_C
5. BRM_N + ZFP3_C
6. BRM_C + ZFP3_N
7. NDUFS8.2-GFP or NDUFS8.1-GFP gene fusions (used as positive control to test the efficiency of the transformation).

YFP fluorescence was detected by confocal microscopy in the Microscopic Imaging Unit of the BRC (collaboration with Dr. Ferhan Ayaydin). Transformation into cultured Arabidopsis cells was reproducible achieved. Fluorescence could be detected in Arabidopsis cell suspensions when the ZFP3 or BRM fusions were introduced into the cells alone (samples 1-4). When combinations BRM_N + ZFP_C and BRM_C + ZFP_N were transformed, fluorescence was similar to the ZFP3 or BRM transformations alone, and enhancement could bot be detected (Figure 2).

Subsequently BiFC was attempted in different experimental system and Nicotiana benthamiana was used for transient expression. GFP-derived fluorescence with BRM and ZFP3 constructs was negligible either alone or in combinations, suggesting that BiFC does not takes place between the ZFP3 and BRM constructs (Figure 3). Transformation of the NDUFS8.2-GFP or NDUFS8.1-GFP gene fusions lead strong fluorescence. These results suggested, that the transient expression was functional, but BiFC, and protein-protewin interactions did not happen between BRM and the ZFP3 constructs.

*Immunoprecipitation and mass spectrometry.*

Pairwise interaction of ZFP3 with subunits of the SWI/SNF complex could not be unequivocally confirmed with Y2H and BiFC technologies. It can happen that *in planta* interactions take place with the multicomponent complex or it needs particular conditions. Special cellular factors may also facilitate such interactions. In order to verify this assumption and identify nuclear proteins which can form complexes with ZFP3, a series of immunoprecipitation (IP) experiments were performed with transgenic plants overexpressing GFP or HA-tagged ZFP3. Overexpressing lines were insensitive to ABA in germination assays, similarly to overexpression of non-tagged ZFP3, therefore we assumed that the epitope-tagged ZFP3 constructs are functional.

In collaboration with the Proteomics Unit of the BRC, 6 IP experiments were performed using GFP and HA-tagged versions of ZFP3, and alltogether 38 samples were analysed. Results of these experiments are summarized in Tables 1-6. ZFP3 could be detected in all experiments, suggesting that experimental procedures were correctly used. The proteins identified in IP samples were very variable. Despite our repeated efforts, no nuclear factors implicated in chromatin remodelling could be identified among the immunoprecipitated proteins. Several proteins have been identified in at least two independent IP experiments, such as Histone deacetylase HDT2, Jacalin-related lectin 11, Chaperonin CPN60-like 2, a putative Gtpase, TPX2 protein, Tubulin alpha-5. These results suggest, that ZFP3 can be involved in protein-protein interactions with different proteins in plant cells, but not with components of the SWI/SNF complex.

**Phosphorylation of ZFP3**

Protein phosphorylation is a common post translational modification of proteins which can interfere with their fonformation, stability and function. In order to study phosphorylation of ZFP3, a series of experiments were made.

*Identification of phosphorylation sites by mass spectrometry*

Mass spectrometry can identify phosphorylated peptides in proteomic surway. Together with experts of thew Proteomics Unit of the BRC, data of 5 samples in 3 experiments were analysed to identify possible ZFP3 phosphorylation sites. Two peptides with 5 possible phosphorylation sites could be identified (Table 7). Phosphorylated peptides are located at the C terminal region of the ZFP3 protein. Structural domain has not been identified in that region.

ZFP3 protein sequence with identified domains and sequence elements

MDASIVSSSTAFPYQDSLNQSIEDEERDVHNSSHELNLIDCIDDTTSIVNESTTSTEQ
KL**FSCNYCQRTFYSSQALGGHQNAH**KRERTLAKRGQRMAASASAFGHPYGFSPL
PFHGQYNNHRSLGIQAHSISHKLSSYNGFGGHYGQINWSRLPFDQQPAIGKFPSM
DNF**HHHHHQMMMM**APSVNSRSNNIDSPSNTGRVLEGSPTLEQWHGDKGLLLSTS
HHEEQQKLDLSLKL

Underlined, bold: **ZnF_C2H2 domain**
Underlined, bold: **low compexity region**
Yellow highlighted sequence: DB peptide 1
Green highlighted sequence: DB peptide 2
Red **S** and **T**: serine and threonine residues with phosphorylation mark.

Schematic domain structure of ZFP3 with predicted phosphorylation sites


*In vitro ZFP3 phosphorylation experiments*

According to mass spectrometry data, ZFP3 protein can be phosphorylated on C-terminal region. To test phosphorylation of ZFP3 in vitro, purified proteins were needed. ZFP3 purification in bacterial system was attempted in several experiments. To produce 6xHis-tagged ZFP3, cDNA was cloned into the protein expression vectors pET28c or pET32Bb and purification was attempted by using protocols of Novagen. Most of the protein was however found in insoluble fractions, even when protocols were modified to increase protein solubility. We have tried several other bacterial expression systems to purify ZFP3, but results were not very encouraging as in most experiments ZFP3 could be identified only in the insoluble fraction, and could not be resolubilized efficiently. While purification of 6xHis-tagged ZFP3 failed, we tried purification of TRX-tagged ZFP3 (fused to thioredoxin tag) with more succes. We got limited amount of TRX-ZFP3 protein, which was subsequently tested for phosphorylation (Figure 4). Immobilized TRX-tagged ZFP3 was used to test phosphorylation with plant extracts derived from different sources: in-vitro grown seedlings, greenhouse-grown plants, stiliques, rosette leaves, using radiolablelled ATP. Unfortunately our efforts failed, phosphorylation of ZFP3 could not be detected in repeated experiments (Figure 5). Due to problems in protein expression, purification and solubility, our experiments could not confirm ZFP3 phosphorylation in vitro.

**Study of ZFP3 chromatin binding**

The fact that ZFP3 overexpression reduces ABA sensitivity of germinating seeds suggested, that ZFP3 controls the expression of ABA regulatory genes in such conditions. In fact, downregulation of *ABI4* and *ABI5* was previously shown in ZFP3 overexpressing seedlings (Joseph et al., 2014). RNAseq transcript profiling indicated that several other ABA-induced genes can be downregulated by ZFP3 (See bellow).

ZFP3 might downregulate ABA-responsive genes either by direct binding to their promoter region and reduce translation initiation as supressor, or interfering upstream processes which can block gene expression. As ABI4 and ABI5 are known TFs which mediate ABA signals in germinating seeds, we assumed, that reduction of their expression by ZFP3 might lead to ABA insensitivity. To clarify this question we tested ZFP3 binding on regulatory regions of *ABI4* and *ABI5* genes using chromatin immunoprecipitation (ChIP) assay. ChIP was made in repeated experiments using Arabidopsis lines which overexpress GFP-tagged ZFP3. Four 5' regions of both genes were selected for PCR amplification of immunoprecipitated chromatin fragments, some of them overlapped with regions which were shown to bind BRM and the SWI/SNF complex (Han et al., 2012, Plant Cell **24:** 4892-4906). Some of the ChIP experiments gave enrichment of one or two such promoter regions, but results were not consistent (Figure 6). In case of *ABI4*, variable degree of enrichment was detected for regions 2 and 3, but results were very variable with low reproducibility. Experiments with *ABI5* gene gave enrichment of a fragment 1.8 kb upstream of the transcription start site in plants which were not treated with ABA. While this results could be reproduced, it is unlikely that a transcription factor binding site so far from the transcription start can have relevance in controlling gene expression. We concluded, that, although ZFP3 might directly regulate some of these and other ABA-related TF genes, it is probably restricted to certain phases of germination. In fact RNAseq transcript profiling did not indicated that these genes are downregulated by ZFP3 in growing plants, suggesting that *ABI4* and *ABI5* might be target of ZFP3 in germinating seeds but not later phases of plant development.

In order to identify ZFP3 binding sites on genomic scale, a ChIP-seq experiment was performed using Arabidopsis plants which overexpress the GFP-tagged ZFP3 factor. Three weeks-old in vitro-grown plants were used in this experiment. Col-0 wild type plants were used as control. ChIP-seq was made in three biological replicates. Evaluation of the sequenced reads could not identify genomic regions with enhanced read frequencies. These results suggest, that ZFP3 either has no direct chromatin binding capacity, or is not active in three weeks-old plants. As next generation sequencing has considerable cost and our financial sources were limited, we could not repeat the experiment with plants of different developmental phase.

**Identification of ZFP3-regulated genes**

In order to identify genes which are regulated by ZFP3 during vegetative growth, whole genome transcript profiling was performed with Col-0 and XVE-ZFP3 plants, using RNAseq technology. A total of 1652 genes had at least 2.5 times difference in transcript abundance between Col-0 and XVE-ZFP3 plants. 6 h estradiol treatment repressed and induced 641 and 571 genes, respectively, while 308 and 421 genes had reduced or enhanced transcript levels after long estradiol exposure (Figure 7).

Gene ontology (GO) classification revealed that many genes which were downregulated by short ZFP3 overexpression, are implicated in cell wall biosynthesis

and organization, root hair differentiation and elongation, response to oxidative stress and to water deprivation. Continuous ZFP3 overexpression repressed less genes and GO terms included aging, response to hypoxia and secondary metabolism. Most GO Cellular component categories were related to cell wall or extracellular region. GO terms related to glucosinolate biosynthesis and sulfur starvation were overrepresented among the genes induced by 6 h ZFP3 overexpression.

RNAseq identified several ZFP3-suppressed genes which respond to water deprivation and ABA, with three to eight times lower transcript levels in XVE-ZFP3 plants than in Col-0 (Figure 5a). ZFP3 overexpression reduced transcript levels of stress-induced *NCED3*, *RAB18* and *RD29A* genes by 40% to 70%, while ZFP3 silencing had only marginal effect on them. ABA was however not or only marginally altered by ZFP3 overexpression or silencing (Figure 8). These results confirmed that in growing plants stress and ABA-induced genes can be repressed by ZFP3 overexpression, but not influenced by silencing.

GO analysis revealed that many genes which are implicated in cell wall biogenesis and modification are overrepresented in ZFP3-repressed gene sets, specially after 6 h of ZFP3 induction (Figure 9A). Such genes encoded enzymes in cell wall formation including cellulose synthase (CSLB), xyloglucan endotransglucosylase /hydrolases (XTH), hydroxyproline-rich proteins such as extensins (EXT), expansins (EXPA), pectine methylestherases (PME), fucosyl transferases (FUT) and casparian strip membrane domain proteins (CASP). Transcript levels of selected *EXPA18, EXT12, RHS12* and *XTH25* genes were repressed in XVE-ZFP3 lines, specially after 6 h of estradiol treatment, while ZFP3 silencing had no clean-cut effect on these genes (Figure 9B). These results demonstrated that a set of genes implicated in cell wall biogenesis or modification are indeed downregulated by ZFP3.

**ABA, salt and osmotic sensitivity of chromatin remodelling mutants.**

To test the sensitivity of chromatin remodelling mutants to osmotic and salt stress and ABA, seeds of Col-0 wild type and *swi73a1, swi73b1, swi3c1, swi3d1* and *brm* mutants were germinated on media supplemented by 0.5 μM ABA, 100 mM NaCl or 200 mM mannitol. Germinated seeds were scored at daily interwals. Germination efficiency of the mutants was similar to wild type on control medium. Germination of the *brm* mutant was very sensitive to ABA, while the other mutants showed similar delay in germination as wild type. Salt and mannitol affected germination in a similar way of the mutant and wild type seed with the exception of brm, which displayed moderate hypersensitivity to these treatments (Figure 10). These results show, that except the ABA hypersensitivity of *brm*, other mutants of the SWI/SNF complex have no differences in stress and ABA sensitivity in germination assays.

**Effect of ZFP3 on ABA regulation**

*ABA responses of ZFP3 overexpressing plants*

ZFP3 was identified due to its capacity to reduce ABA sensitivity of seed germination, suggesting that this factor is a negative regulator of ABA signals. Overexpression of similar ZFP factors could also confer ABA insensitivity to germinating seeds, indicating certain degree of functional redundancy in closely-related ZFPs (Joseph, et al., 2014). To test possible epistasis with known ABA signaling factors, ABA responses of XVE-ZFP3 plants were tested not only in Col-0, but also in the ABA insensitive *abi4* and *abi5* mutant backgrounds. On standard

growth conditions rosette sizes of all genotypes were similar to Col-0, except the constitutively overexpressing 35S-ZFP3 plants, which had around 35% smaller rosettes than wild type ones. On estradiol-containing media Col-0, *abi4* and *abi5* plants were similar to plants grown on control conditions, while plants with XVE-ZFP3 construct were 30 to 60% smaller (Figure 11).

Root lengths of XVE-ZFP3 plants were 15 to 20% smaller than non-transgenics on standard growth medium. Inhibition of root elongation by increasing concentration of ABA was stronger in ZFP3 overexpressing plants without clear differences between the Col-0 and *abi4* or *abi5* mutants. These results show, that ZFP3 does not confer ABA insensitivity to overexpressing plants during post-germination growth. Additive nature of ABA treatment and ZFP3 overexpression on growth reduction suggests that ZFP3 controls vegetative growth parallel to ABA regulation.

*ABA, salt and mannitol sensitivity of zfp mutants and ZFP3 overexpressing plants*

T-DNA insertion mutants were acquired for ZFP3 and closely related ZnF genes: *ZFP1*, *ZFP3*, *ZFP4*, *ZFP5* and *ZFP8*. Testing the expression of these genes in the mutants however revealed that some of them were not real knockouts. Nevertheless mutants were crossed to generate multiple lines and were tested in germination assay for ABA, salt and mannitol sensitivities. Mutants and ZFP3 overexpressing lines (35S-ZFP3-HA and 35S-ZFP3-GFP) germinated in similar efficiency when cultured on standard ½ MS medium and reached nearly 100% germination within 4 days after plating. The *zfp1/zfp3/zfp4* triple mutan and the 35S-ZFP3-HA line were slightly delayed in germination in control conditions. As expected, ABA reduced germination considerably of all lines. Germination of the *zfp4* mutant and the *zfp1/zfp4, zfp4/zfp8* double and *zfp1/zfp3/zfp4* triple mutants were more supressed, while the two ZFP3 overexpressing lines germinated faster than wild type. The other mutants germinated at rates similar to Col-0. Salt and mannitol reduced germination efficiencies, but the differences between the genotypes were not as remarkable as with ABA. The *zfp1/zfp3/zfp4* triple triple mutant was more affected by both treatments. It is notable, that ZFP3 overexpressing lines were not better, and ZFP3-HA was clearly inferior than Col-0 in salt and mannitol assays (Figure 12). These results showed, that except *zfp4* the other mutations had not affected germination efficiency in standard or stress conditions. ABA sensitivity of *zfp4* mutant was remarkable, while the overexpressing lines were ABA insensitive.

*Proline accumulation*

Proline accumulation is a characteristic stress response of higher plants, and is controlled by light and ABA-dependent signals during salt or osmotic stress. To find out whether ZFP3 influences proline metabolism, *in vitro* grown single and multiple *zfp* mutants and ZFP overexpressing plants were treated with and without 50 μM ABA and proline levels were measured after two days. No difference was found in proline levels of the mutants and ZFP3 overexpressing plants. While ABA treatment resulted in enhanced proline accumulation genotype-dependent difference could not be established. Proline levels in SWI/SNF mutants were comparable to wild type plants. ABA treatment did not lead to significant differences between these genotypes (Figure 13). Although ZFP3 overexpressing plants were insensitive to ABA and *brm* is hypersensitive to ABA in germination tests, such difference in ABA sensitivity is apparently restricted to germination and has no influence on ABA-controlled metabolic processes such as proline accumulation.

**ZFP3 modulates growth and development.**

*Plant phenotyping*

As T-DNA insertion mutants were not genuine knockouts, knock-down lines were generated by artificial microarray technology and *ZFP1, ZFP3, ZFP4* and *ZFP7* genes were silenced with 18% to 36% efficiency. Growth and morphology of soil-grown 35S-ZFP3 plants, amiR silenced lines and mutants were monitored in an automatic phenotyping platform. ZFP3 overexpressing plants frequently displayed growth defects, had wrinkled leaves and flowered with some delay than Col-0 plants, while the *zfp3* and *zfp4* mutants were similar to wild type (Figure 2a). Image analysis revealed that rosette sizes of soil-grown ZFP3 overexpressing plants were 25 to 70% smaller than Col-0 plants, depending on the transgenic line analysed. Insertion mutants were similar to wild type plants (*zfp3*), or were smaller (*zfp4*). Silencing of *ZFP1, ZFP3, ZFP4* and *ZFP7* genes had no dramatic consequence on plant phenotype and growth (Figure 14).

*Scanning electron microscopy of leaf epidermis*

Scanning electron microscopy was used to study leaf epidermal cells of ZFP3 overexpressing and wild type plants. 35S-ZFP3 cells were generally smaller than wild type, and had less complex shape (Figure 3a). Average cell areas of 35S-ZFP3 cells were 30 to 60% smaller than wild type, and had less complex cell form than wild type. Smaller cell size and defects in cell differentiation of ZFP3 overexpressing plants can explain the phenotypic abnormalities observed in developing plants (Figure 15).

*Root hair growth is reduced by ZFP3 overexpression*

Defects in cell wall formation can affect cell differentiation, elongation in root cells. As numerous root hair specific (RHS) genes were also downregulated by ZFP3, we have studied root hair formation in detail. Root hairs of 35S-ZFP3 plants were 30 to 60% shorter than in Col-0, while in zfp3amiR plants they were either similar or slightly longer. ZFP3 overexpression reduced the number of root hairs, suggesting that root hair initiation is also affected (Figure 16).

Estradiol-inducible overexpression of *ZFP1, ZFP3, ZFP4* and *ZFP7* resulted in 40% to 60% reduction of root hair lengths. These results demonstrate, that ZFP3 and the most closely related ZFP factors negatively regulate root hair formation. Silencing of single ZFP genes had no effect on root hair lengths suggesting functional redundancy of closely related ZFP genes as closely related genes can at least partially compensate the defect of one ZFP gene.

**Conclusions, additional research.**

As conclusion, our study highlighted the importance of the C2H2 ZnF protein ZFP3 in plant growth, particularly in root hair development. Defects in cell differentiation can be the consequence of inhibition of regulatory genes such as RHD6 or RSL4, leading to reduced expression of structural genes implicated in cell wall formation and modification (Figure 17). We could therefore demonstrate that ZFP3 and the most closely related ZFP factors are important regulators of cell growth and differentiation which in fact has consequences on plant development (Benyó et al., 2021).

Besides pursuing our aims to characterize the function of ZFP3 and related ZnF proteins, find link with chromatin remodelling machinery and other regulatory mechanisms and identify genes controlled by these factors, we performed experiments which in some points are related to the main topic of the project. Here we showed, that ZFP3 regulate root growth and root hair development (Benyó et al., 2021). Root growth is controlled by several plant hormones with auxin as the main regulator. We showed that a CDPK-related kinase (CRK5) is important in control of auxin transport by phosphorylating PIN transporters which modulates their activitis and therefore root growth and gravitropic response (Cséplő et al., 2021). The same CRK5 kinase regulated hypocotyl hook development during skotomorphogenesis and embryogenesis through modulation polar auxin transport (Baba et al., 2019a, 2019b). Our earlier studies revealed light-dependent control of hypocotyl development was influenced by ZFP3, which promoted red light signals and contained hypocotyl elongation (Joseph et al., 2014). Red light is needed for proline biosynthesis in salt-treated Arabidopsis plants, which is regulated by bZIP factor HY5, binding to the promoter of the P5CS1 gene (Kovács et al., 2018). Proline biosynthesis is controlled by stress, light, ABA, energy status and developmental signals (Alvarez et al., 2021). Although ZFP3 can control ABA sensitivity and plant development, proline accumulation does not seem to be regulated by this factor,

**References**

**Bruex A, Kainkaryam, R. M., Wieckowski, Y., Kang, Y. H., Bernhardt, C., Xia, Y., Zheng, X., Wang, J. Y., Lee, M. M., Benfey, P., Woolf, P. J., Schiefelbein, J.** (2012) A gene regulatory network for root epidermis cell differentiation in Arabidopsis. PLoS Genetics **8:** e1002446

**Han SK, Sang Y, Rodrigues A, Biol F, Wu MF, Rodriguez PL, Wagner D** (2012) The SWI2/SNF2 chromatin remodeling ATPase BRAHMA represses abscisic acid responses in the absence of the stress stimulus in Arabidopsis. Plant Cell **24:** 4892-4906

**Joseph MP, Papdi C, Kozma-Bognar L, Nagy I, Lopez-Carbonell M, Rigo G, Koncz C, Szabados L** (2014) The Arabidopsis ZINC FINGER PROTEIN3 Interferes with Abscisic Acid and Light Signaling in Seed Germination and Plant Development. Plant Physiol **165:** 1203-1220

**Publications**

Andrási N, Rigó G, Zsigmond L, Pérez-Salamó I, Papdi C, Klement E, Pettkó-Szandtner A, Baba AI, Ayaydin F, Dasari R, Cséplő A, Szabados L (2019) The mitogen-activated protein kinase 4-phosphorylated heat shock factor A4A regulates responses to combined salt and heat stresses. J Exp Bot 70: 4903-4918

Baba AI, Andrasi N, Valkai I, Gorcsa T, Koczka L, Darula Z, Medzihradszky KF, Szabados L, Feher A, Rigo G, Cseplo A (2019) AtCRK5 Protein Kinase Exhibits a Regulatory Role in Hypocotyl Hook Development during Skotomorphogenesis. Int J Mol Sci 20: 3432

Kovacs H, Aleksza D, Baba AI, Hajdu A, Kiraly AM, Zsigmond L, Toth SZ, Kozma-Bognar L, Szabados L (2019) Light Control of Salt-Induced Proline Accumulation Is Mediated by ELONGATED HYPOCOTYL 5 in Arabidopsis. Front Plant Sci 10: 1584

Baba AI, Valkai I, Labhane NM, Koczka L, Andrasi N, Klement E, Darula Z, Medzihradszky KF, Szabados L, Feher A, Rigo G, Cseplo A (2019) CRK5 Protein

Kinase Contributes to the Progression of Embryogenesis of Arabidopsis thaliana. Int J Mol Sci 20: 6120

Cséplő Á, Zsigmond, L, Andrási, N, Baba, A.i., Labhane, N., Pető, A., Kolbert, Zs., Kovács, H.E., Steinbach, G., Szabados, L., Fehér, A., Rigó, G. (2021) The AtCRK5 Protein Kinase Is Required to Maintain the ROS NO Balance Affecting the PIN2-Mediated Root Gravitropic Response in Arabidopsis. International Journal of Molecular Sciences 22: 1200716

Alvarez ME, Savouré, A, Szabados, L. (2021) Proline metabolism as regulatory hub. Trends Plant Sci (PLANTS-S-21-00073, in revision)

Benyó D, Bató, E., Faragó, D., Rigó, G., Domonkos, I., Labhane, N., Zsigmond, L., Nagy, I., Szabados, L. (2021) The Arabidopsis Zinc Finger Protein 3 and related ZFPs regulate cellular differentiation and plant growth. New Phytology, (NPH-MS-2021-36823, in revision).

**Results disseminated in Conferences**

Szabados L, Rigó G, Valkai I, Faragó D, Kiss E, Koncz Cs, Van Houdt S, Van de Steene N, Hannah MA (2017) TASARD 2017 Conference, New Delhi, India.

Dávid Aleksza, Hajnalka Kovács, Laura Zsigmond, Gábor V. Horváth, Arnould Savouré, László Szabados (2017) National Symposium on Genetics, Osmania University, Hyderabad, India.

Dániel Benyó, Mary Prathiba Joseph, Nitin Labhane and László Szabados (2017) ZFP3 and flowering time regulation in Arabidopsis. Straub Napok, 2017 május, Szeged.

László Szabados, Gábor Rigó, Ildikó Valkai, Dóra Faragó, Edina Kiss, Csaba Koncz, Sara Van Houdt, Nancy Van de Steene, Matthew A. Hannah (2017) 19th National Biotechnology Congress with International Participation, Eskisehir, Turkey, December 1-3, 2017

Abu Imran Baba, Gabor Rigó, Ferhan Ayaydin, Norbert Andrási, Ateeq Ur Rehman, Janos Urbancsok, Laura Zsigmond, Ildiko Valkai, Imre Vass, Taras Pasternak, Klaus Palme, Laszlo Szabados and Ágnes Cséplő (2018) Plant Biology Europe FESPB/EPSO Congress 2018, Copenhagen, Denmark,

Abu Imran Baba, Ildikó Valkai, Nitin Labhane, Norbert Andrási, Laura Zsigmond, László Szabados, Attila Fehér, Gábor Rigó and Ágnes Cséplő (2019) Hungarian Molecular Life Sciences 2019 Conference, Eger.

Dávid Aleksza, Hajnalka Kovács, Abu Imran Baba, Anita Hajdu, Laura Zsigmond, Szilvia Zita Tóth, Anna Mária Király, László Kozma-Bognár, László Szabados (2019) Hungarian Molecular Life Sciences 2019 Conference, Eger.

László Szabados, Norbert Andrási, Gábor Rigó, Laura Zsigmond, Eva Klement, Aladár Pettkó-Szandtner, Abu Imran Baba, Ferhan Ayaydin, Ágnes Cséplő, Imma Pérez-Salamó, Csaba Papdi (2019) Impact of Nuclear Domains On Gene Expression and Plant Traits, El-Escorial, Spain,

László Szabados, Dóra Faragó, Laura Zsigmond, Dániel Benyó, Ferhan Ayaydin, Rubén Alcazar, Gábor Rigó (2020) Plant Abiotic Stress Tolerance VI, Vienna International Science Conferences and Events Association (VISCEA), February 21-22, 2020, Vienna, Austria.

## Tables

**Table 1. Immunoprecipitation experiment 1.**
ZFP3-GFP construct was used for Imunoprecipitation. Proteins immunoprecipitated samples were identified with mass spectrometry. Date: 2017.05.18

| Acc # | Gene | Protein Name | Rel. Score |
|---|---|---|---|
| Q0WT56 | **ZFP3** | **ZFP3 zinc finger protein** | 120 |
| O65572 | CCD1 | Carotenoid 9,10(9',10')-cleavage dioxygenase 1 | 40 |
| P0DKC3 | PGLP1A | Phosphoglycolate phosphatase 1A, chloroplastic | 40 |
| Q94K71 | CBBY | Haloacid dehalogenase-like hydrolase (HAD) superfamily protein, CBBY-like protein | 30 |
| Q9LTR2 | TGD2 | Protein TRIGALACTOSYLDIACYLGLYCEROL 2, chloroplastic | 30 |
| Q9SR77 | At3g10130 | Heme-binding-like protein At3g10130, chloroplastic | 30 |
| P82538 | PPL1 | PsbP-like protein 1, chloroplastic | 30 |
| O81014 | ISPE | 4-diphosphocytidyl-2-C-methyl-D-erythritol kinase, chloroplastic | 20 |
| Q8H0V3 | At1g08110 | Lactoylglutathione lyase | 20 |
| P82873 | TOM20-2 | Mitochondrial import receptor subunit TOM20-2 | 20 |
| O23403 | PPD1 | PsbP domain-containing protein 1, chloroplastic | 20 |
| Q7M1W7 | | Protein QA100047 (Fragment) | 20 |
| O22126 | FLA8 | Fasciclin-like arabinogalactan protein 8 | 11 |
| Q9FV71 | E2FB | Transcription factor E2FB | 10 |
| Q93Z49 | MHJ24.11 | AT5g64130/MHJ24_11 | 10 |
| Q0WW83 | At5g57850 | Branched-chain amino acid aminotransferase like protein | 10 |
| Q9SUR6 | CORI3 | Cystine lyase CORI3 | 10 |
| P18612 | KIN1 | Stress-induced protein KIN1 | 10 |
| Q9M2V1 | NCA1 | Protein NCA1 | 10 |
| Q9FYC2 | PAO | Pheophorbide a oxygenase, chloroplastic | 10 |
| Q9SZC9 | PAA1 | Copper-transporting ATPase PAA1, chloroplastic | 10 |
| Q9FNJ9 | At5g22620 | Probable 2-carboxy-D-arabinitol-1-phosphatase | 10 |
| Q8L475 | At1g74640 | Alpha/beta-Hydrolases superfamily protein | 10 |
| Q42335 | | MIF homologue (Fragment) | 10 |
| P55852 | SUMO1 | Small ubiquitin-related modifier 1 | 10 |
| P11490 | PETE | Plastocyanin minor isoform, chloroplastic | 10 |
| A0A178VIV9 | At3g42620 | TAC10 | 10 |
| Q8L9F4 | | Uncharacterized protein | 10 |
| Q9CAC8 | F24D7.19 | At1g63610 | 10 |
| Q8LAD0 | PDX2 | Probable pyridoxal 5'-phosphate synthase subunit PDX2 | 10 |
| Q42307 | | Protein kinase receptor-like (Fragment) | 10 |
| Q9LIN5 | EIF4B1 | Eukaryotic translation initiation factor 4B1 | 10 |
| A0A178UIH1 | At5g04000 | Uncharacterized protein | 10 |
| decoy | F18P9_90 | Uncharacterized protein F18P9_90 | 10 |
| P55217 | CGS1 | Cystathionine gamma-synthase 1, chloroplastic | 10 |
| decoy | At2g29880 | Uncharacterized protein | 10 |

**Table 2. Immunoprecipitation experiment 2.**
ZFP3-HA construct was used for Imunoprecipitation. Proteins immunoprecipitated samples were identified with mass spectrometry. Date: 2017.05.18

| Acc # | Gene | Protein Name | Rel. Score |
|---|---|---|---|
| Q0WT56 | **ZFP3** | **ZFP3 zinc finger protein** | 60 |
| decoy | At5g44720 | Uncharacterized protein | 30 |
| decoy | At4g16730 | Cfm3b | 20 |
| Q56ZZ7 | GLT1 | Glucose transporter 1, pglct, plastidic glc translocator | 10 |
| Q9FZ43 | F6I1.17 | 7-dehydrocholesterol reductase-like protein | 10 |
| B0LYL3 | BGL1 | Beta-glucosidase 1 (Fragment) | 10 |
| Q9SIC8 | At2g31410 | Coiled-coil protein | 10 |
| decoy | At1g59580 | Uncharacterized protein | 10 |
| Q8L9Z7 | | Uncharacterized protein | 10 |
| A0A178VL95 | At2g32250 | Ubq7 | 10 |
| decoy | At3g11770 | Uncharacterized protein | 10 |
| decoy | ycf1 | Protein TIC 214 | 10 |
| decoy | At3g49230 | Uncharacterized protein | 10 |

**Table 3. Immunoprecipitation experiment 3.**
ZFP3-GFP construct was used for Imunoprecipitation. Proteins immunoprecipitated samples were identified with mass spectrometry. Date: 2018.04.30

| Acc # | Gene | Protein Name | Rel. Score |
|---|---|---|---|
| Q0WT56 | **ZFP3** | **ZFP3 zinc finger protein** | 110 |
| Q5XF82 | JAL11 | Jacalin-related lectin 11, Mannose-binding lectin protein | 70 |
| Q93ZM7 | HSP60-3A | Chaperonin CPN60-like 2, HSP60-3A | 20 |
| Q9C7C0 | DER, EMB2738 | Gtpase, putative; EMBRYO DEFECTIVE 2738 | 20 |
| Q6NPR7 | At1g29470 | Probable methyltransferase PMT24 | 20 |
| Q9ZNT3 | ADF5 | Actin-depolymerizing factor 5 | 20 |
| Q949Y5 | EGY1 | Probable zinc metalloprotease EGY1, chloroplastic | 20 |
| Q3MK93 | ECT2 | Evolutionarily conserved c-terminal region 2 | 11 |
| O65538 | F4D11.190 | Glycoprotein family protein | 10 |
| Q56WH4 | HDT2, HD2 | Histone deacetylase HDT2 | 10 |
| Q9SJ62 | WDL4, TPX2 | TPX2 protein, Protein WVD2-like 4 | 10 |
| Q56YZ2 | TIUA5,TUA3 | TUBULIN ALPHA-5, Tubulin alpha-2/alpha-4 chain | 10 |
| Q9SJU9 | GC1 | Epimerase family protein SDR39U1 homolog, chloroplastic | 10 |
| decoy | At2g02023 | Uncharacterized protein | 10 |
| decoy | HR4 | Homolog of rpw8 4 | 10 |
| decoy | At5g45720 | Protein STICHEL-like 4 | 10 |

**Table 4. Immunoprecipitation experiment 4.**
ZFP3-HA construct was used for Imunoprecipitation. Proteins immunoprecipitated samples were identified with mass spectrometry. Date: 2018.04.30

| Acc # | Gene | Protein Name | Rel. Score |
|---|---|---|---|
| Q0WT56 | **ZFP3** | **ZFP3 zinc finger protein** | 110 |
| Q5XF82 | JAL11 | Jacalin-related lectin 11, Mannose-binding lectin protein | 110 |
| O65538 | F4D11.190 | Glycoprotein family protein | 80 |
| O23290 | RPL36AA | 60S ribosomal protein l36a | 80 |
| P29525 | OLE1 | Oleosin 18.5 kda | 60 |
| Q945N1 | MXI22.1 | Galactose oxidase/kelch repeat superfamily protein | 50 |
| Q9ZVU4 | At1g55450 | S-adenosyl-L-methionine-dependent methyltransferase | 50 |
| Q56WH4 | HDT2, HD2, | Histone deacetylase HDT2 | 30 |
| Q56ZZ7 | GLT1 | Glucose transporter 1, pglct, plastidic glc translocator | 30 |
| Q9M8Z5 | NSN1 | Guanine nucleotide-binding protein-like NSN1 | 30 |
| O80358 | FPG1, MMH1 | Formamidopyrimidine-DNA glycosylase | 30 |
| Q8L606 | TPR-like | Tetratricopeptide repeat (TPR)-like superfamily protein | 30 |
| Q9FG73 | OLI2 | Oligocellula 2, trm4c, trna methyltransferase 4c | 30 |
| P15460 | AT2S4, SESA4 | 2S seed storage protein 4, SEED STORAGE ALBUMIN | 30 |
| Q9SUA1 | DEK3 | DEK domain-containing chromatin associated protein | 21 |
| Q93ZM7 | HSP60-3A | Chaperonin CPN60-like 2, HSP60-3A | 20 |
| Q9LEU5 | At5g10950 | Tudor/PWWP/MBT superfamily protein | 20 |
| Q93ZG9 | FKBP53 | Peptidyl-prolyl cis-trans isomerase FKBP53 | 20 |
| Q9M7Q7 | PCNA | Proliferating cellular nuclear antigen 1 | 20 |
| Q39165 | At5g40420 | Oleosin 21.2 kda | 20 |
| Q93ZB6 | HEME1 | Uroporphyrinogen decarboxylase 1, chloroplastic | 20 |
| Q941L0 | CESA3 | Cellulose synthase A catalytic subunit 3 [UDP-forming] | 20 |
| Q9FMS0 | MWD9.11 | At5g22320/mwd9_11 | 11 |
| Q9C7C0 | DER, EMB2738 | Gtpase, putative; EMBRYO DEFECTIVE 2738 | 10 |
| Q9SJ62 | WDL4, TPX2 | TPX2 protein, Protein WVD2-like 4 | 10 |
| Q56YZ2 | TIUA5, TUA3, | TUBULIN ALPHA-5, Tubulin alpha-2/alpha-4 chain | 10 |
| Q9LVF2 | At3g21540 | Transducin family protein / WD-40 repeat family protein | 10 |
| P32068 | ASA1 | Anthranilate synthase alpha subunit 1, chloroplastic | 10 |
| Q5XF06 | TIM44-2 | Mitochondrial import inner membrane translocase TIM44-2 | 10 |
| Q9S7W4 | F17A17.6 | At3g07720/F17A17_6 | 10 |
| Q8RWB7 | At1g29790 | Cellulose synthase like c5 | 10 |
| Q42529 | TSA1 | Tryptophan synthase alpha chain, chloroplastic | 10 |
| Q9M1S4 | T5N23_120 | Dentin sialophosphoprotein-like protein | 10 |
| A0A178VNE0 | At2g37440 | Ribosome biogenesis protein BOP1 homolog | 10 |
| decoy | At4g22666 | Bifunctional inhibitor/lipid-transfer protein/seed storage 2S albumin superfamily protein | 10 |
| Q8S8F8 | GEM | GLABRA2 expression modulator | 10 |
| decoy | At2g23400 | Alkyl transferase | 10 |
| Q9STH7 | At4g12340 | At4g12340/t4c9_180 | 10 |
| decoy | AOP2 | 2-oxoglutarate-dependent dioxygenase (Fragment) | 10 |
| P15458 | AT2S2 | 2S seed storage protein 2 | 10 |

**Table 5. Immunoprecipitation experiment 5.**
ZFP3-GFP construct was used for Imunoprecipitation. Proteins immunoprecipitated samples were identified with mass spectrometry. Date: 2019.06.16

| Acc # | Gene | Protein Name | **Rel. Score** |
|---|---|---|---|
| Q0WT56 | At5g25160 | ZFP3 zinc finger protein | 76 |
| P42212 | GFP | Green fluorescent protein | 48 |
| Q9CAV0 | RPS3AA | 40S ribosomal protein S3a-1 | 22 |
| Q9LS94 | RABG3F | Ras-related protein RABG3f | 20 |
| Q9LJR2 | LEC | Lectin-like protein LEC | 18 |
| Q41932 | PSBQ2 | Oxygen-evolving enhancer protein 3-2, chloroplastic | 16 |
| Q93V56 | PPA1 | Soluble inorganic pyrophosphatase 1, PPA1 | 14 |
| Q9SL42 | PIN1 | Peptidyl-prolyl cis-trans isomerase Pin1, | 14 |
| O22860 | RPL38A | 60S ribosomal protein L38 | 14 |
| Q8LC83 | RPS24B | 40S ribosomal protein S24-2 | 14 |
| O22254 | RPL18A | Putative 60S ribosomal protein L18-1 | 12 |
| Q9ZWT2 | CYTB5-D | Cytochrome B5 isoform D, CYTB5-D | 12 |
| P56761 | psbD | Photosystem II D2 protein | 12 |
| Q9LXG1 | RPS9B | 40S ribosomal protein S9-1 | 11 |
| Q7DLK3 | | LEA76 homolog (Fragment) | 10 |
| Q9C909 | RBG5 | Glycine-rich RNA-binding protein 5, mitochondrial | 10 |

**Table 6. Immunoprecipitation experiment 6.**
ZFP3-HA construct was used for Imunoprecipitation. Proteins immunoprecipitated samples were identified with mass spectrometry. Date: 2019.06.16

| Acc # | Gene | Protein Name | **Rel. Score** |
|---|---|---|---|
| Q9FGT8 | TIL | Temperature-induced lipocalin-1 | 18 |
| Q9C551 | RH5 | DEAD-box ATP-dependent RNA helicase 5, RH5 | 18 |
| Q8H7F3 | | Aspartic_peptidase_A1, APA1 | 12 |
| Q9LJ97 | RAB28 | Late embryogenesis abundant protein 31, RAB28 | 12 |
| Q0WT56 | At5g25160 | **ZFP3 zinc finger protein** | 10 |
| O49597 | HMGB5 | High mobility group B protein 5, HMGB5 | 8 |

**Table 7. Phosphopeptides identified in ZFP3 protein by mass spectrometry.**

| Acc # | % Cov | DB Peptide | Variable Mods | Protein Mods |
|---|---|---|---|---|
| Q0WT56 | 40.4 | SNNIDSPSNTGR | Phospho@6\|8 | Phospho@193\|195 |
| Q0WT56 | 40.4 | SNNIDSPSNTGR | Phospho@8\|10 | Phospho@195\|197 |
| Q0WT56 | 40.4 | SNNIDSPSNTGR | Phospho@6\|8\|10 | Phospho@193\|195\|197 |
| Q0WT56 | 40.4 | VLEGSPTLEQWHGDK | Phospho@5=7 | Phospho@204=7 |
| Q0WT56 | 40.4 | VLEGSPTLEQWHGDK | Phospho@5=11 | Phospho@204=11 |
| Q0WT56 | 40.4 | VLEGSPTLEQWHGDK | Phospho@5=10 | Phospho@204=10 |

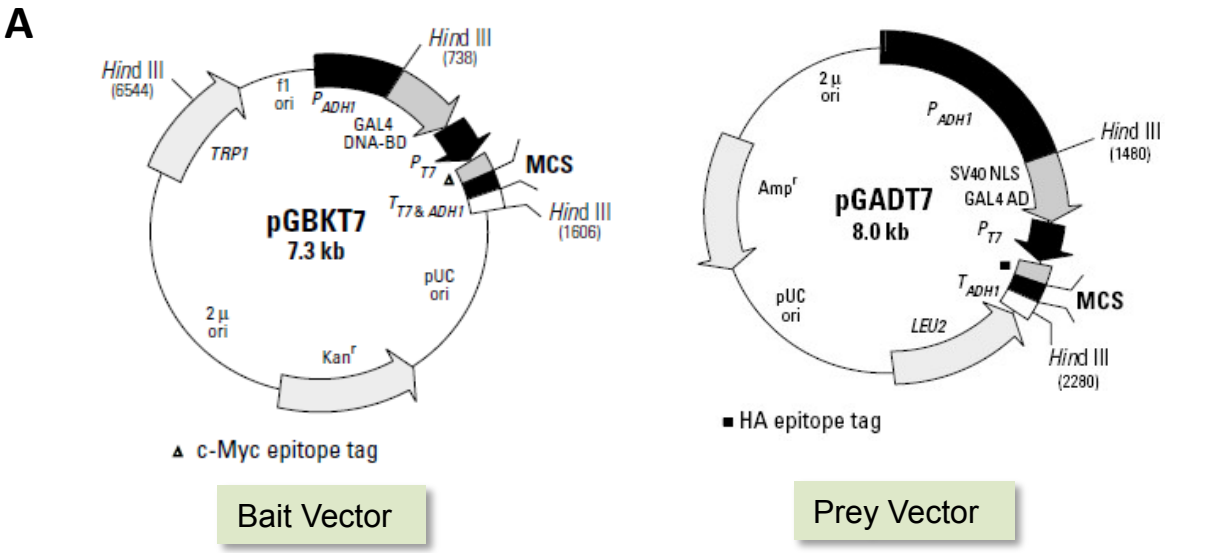


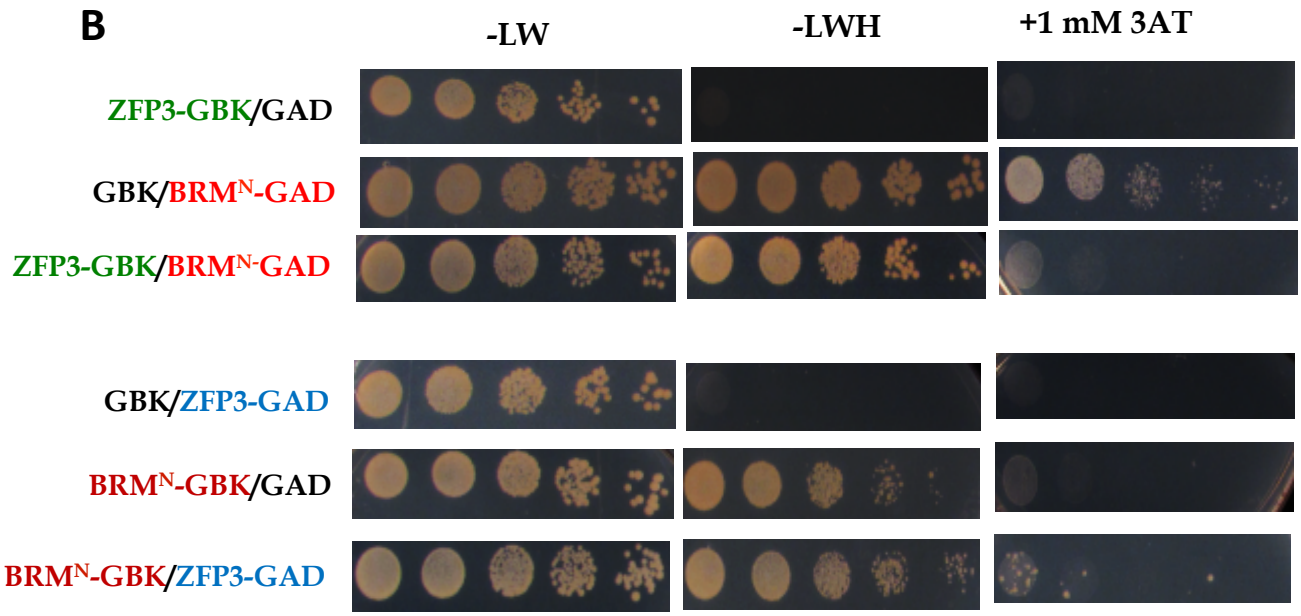


**Figure 1.** Yeast two hybrid system to test interaction of ZFP3 and subunits of the SWI/SNF chromatin remodelling complex. A) Vectors used in the Y2H experiments. B) Interaction test of ZFP3 and Brahma (BRM) in the PJ69-4a yeast strain. Note self activation of BRM constructs. Growth was enhanced slightly in combination of ZFP3 and BRM, suggesting that these factors do not interact or their interaction is weak in the Y2H system.

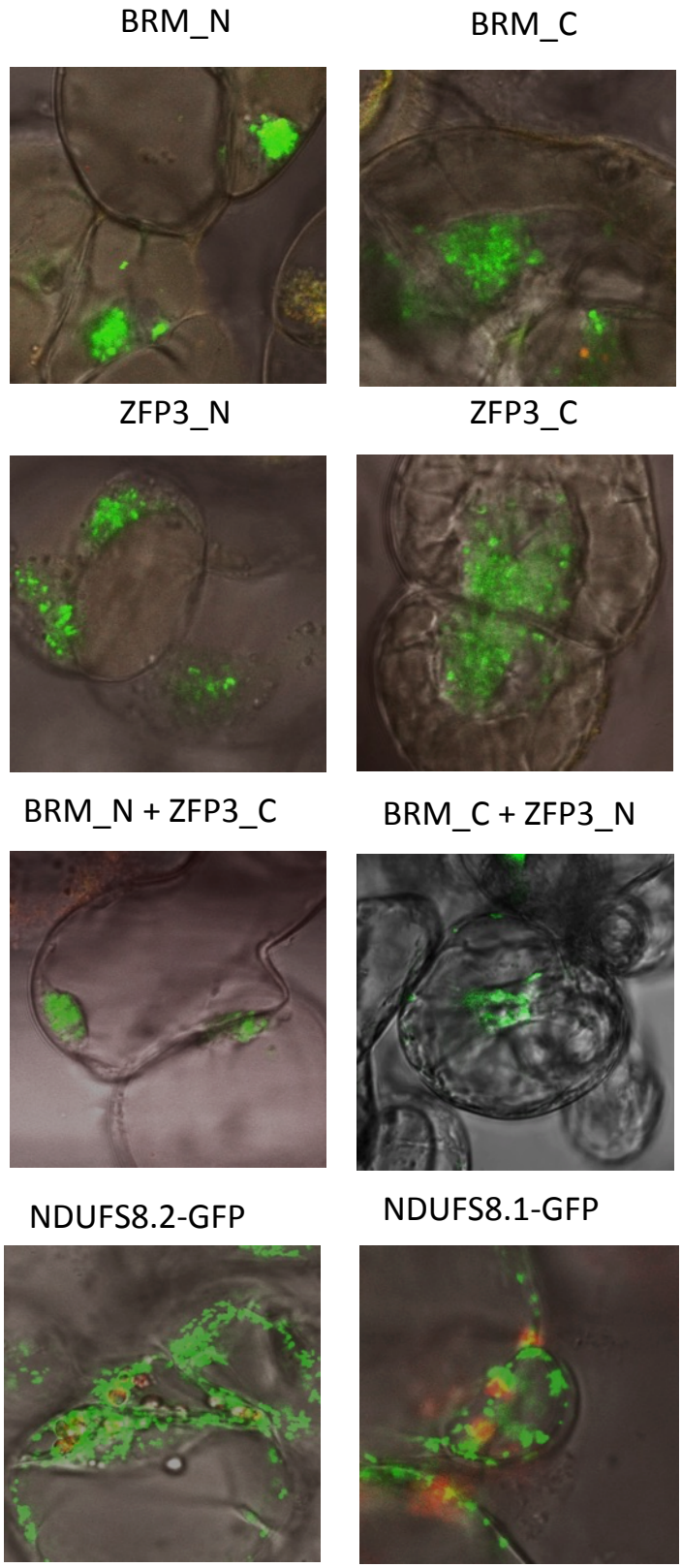


**Figure 2.** BiFC assay in Arabidopsis cell suspension cultures. Strong backlground fluorescence could be detected when single constructs were introduced into the Arabidopsis cells (BRM_N, BRM_C, ZFP3_N, ZFP3_C). Fluorescence had similar intensity when BRM and ZFP3 constructs were introduced into the cells together (BRM_N + ZFP3_C, BRM_C + ZFP3_N). BiFC data could not confirm interaction of BRM and ZFP3.

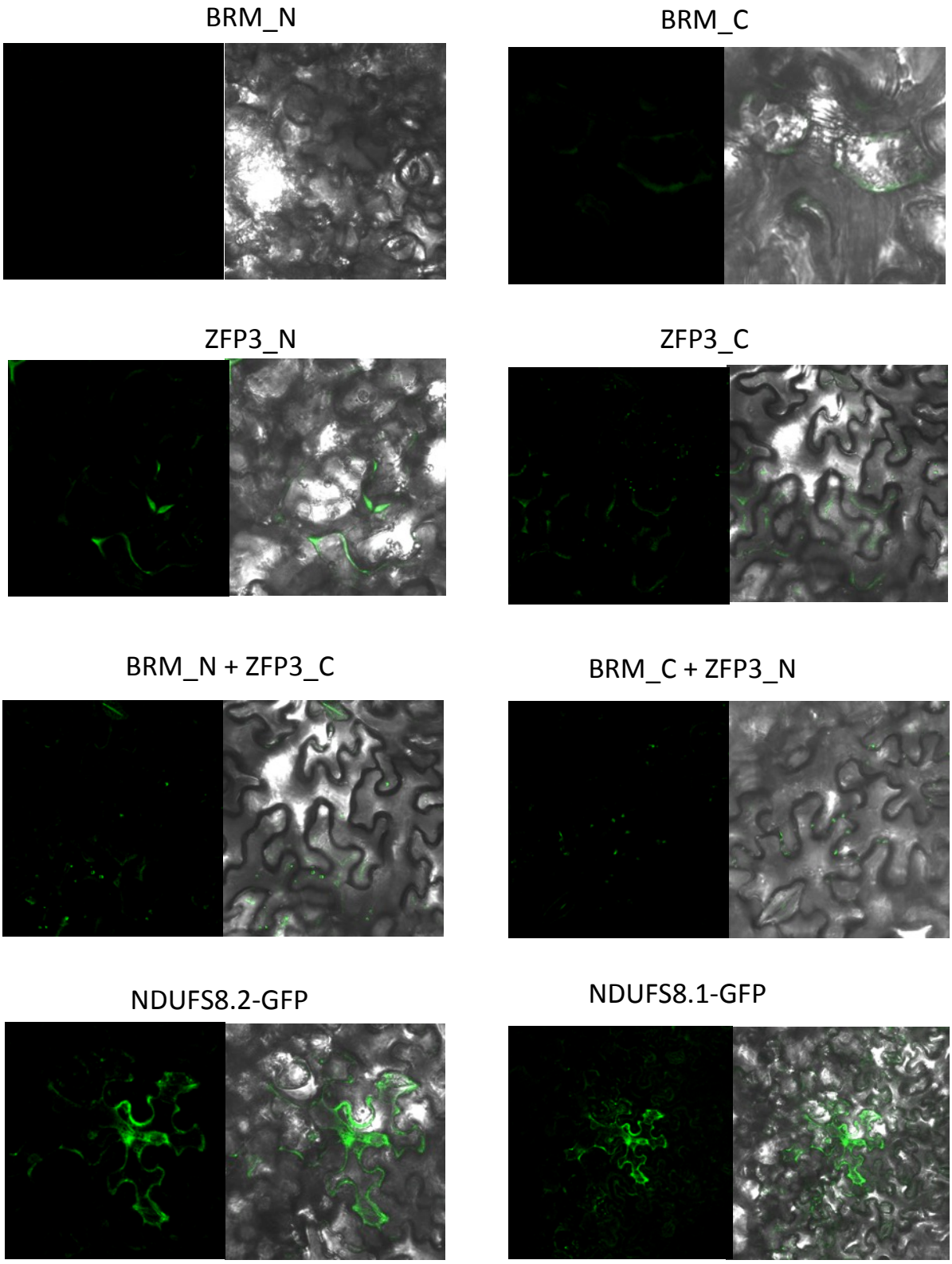


**Figure 3.** BiFC assay in *N. benthamiana* leaf cells. Fluorescence could not be detected or was very weak in all combinations of BRM and ZFP3 constructs. Control GFP constructs (NDUFS8.2-GFP, NDUFS8.1-GFP) displayed strong fluorescence showing that the transient expression system was working.

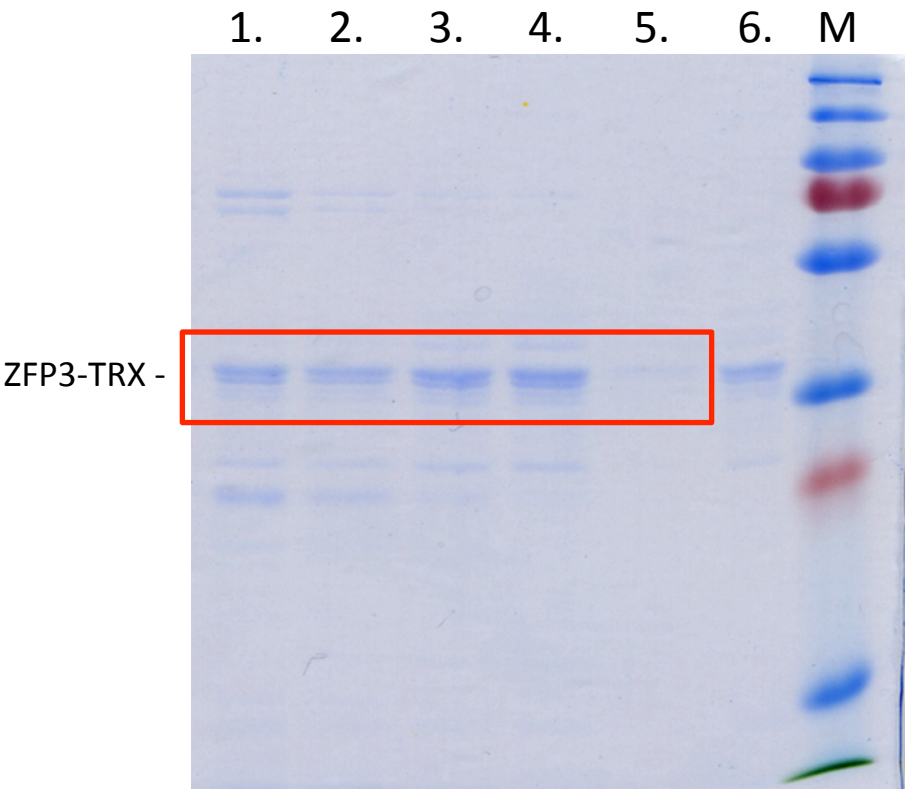


**Figure 4.** Purification of ZFP3 in a bacterial expression system. Isolation of TRX-fused ZFP3 with Ni-NTA matrix. Lanes 1-5: elution with increasing imidazole concentration, lane 6: boiled Ni-NTA matrix.

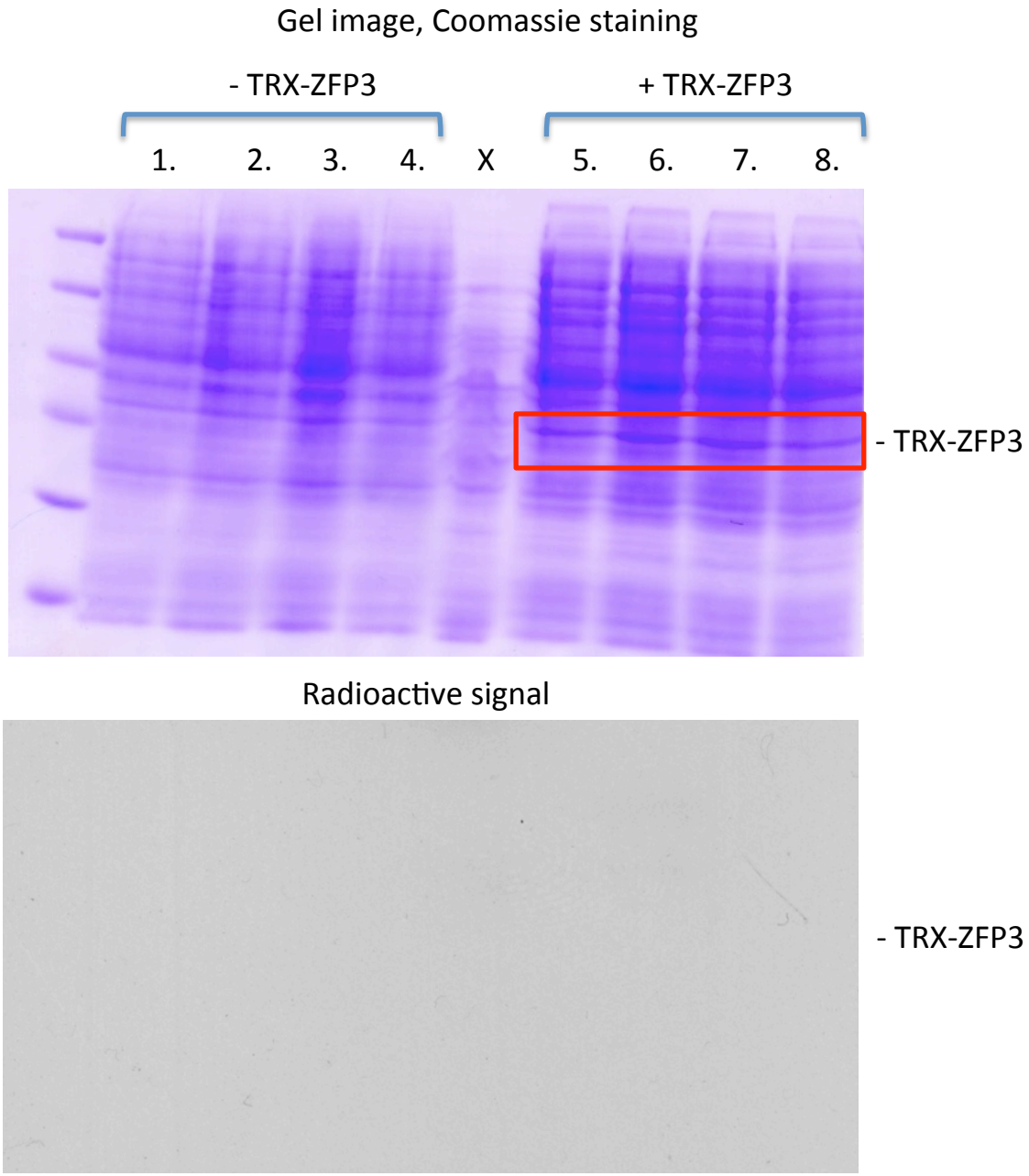


**Figure 5.** Phosphorylation of Ni-NTA-immobilized ZFP3-TRX. Plant extracts: 1,5: in vitro-grown seedlings, 2,6: flower buds, siliques, 3,7: stems, 4,8: rosette leaves. Samples were incubated in the presence of radioactively labelled ATP, separated on PAGE and exposed to X-ray film. No signal could be detected.

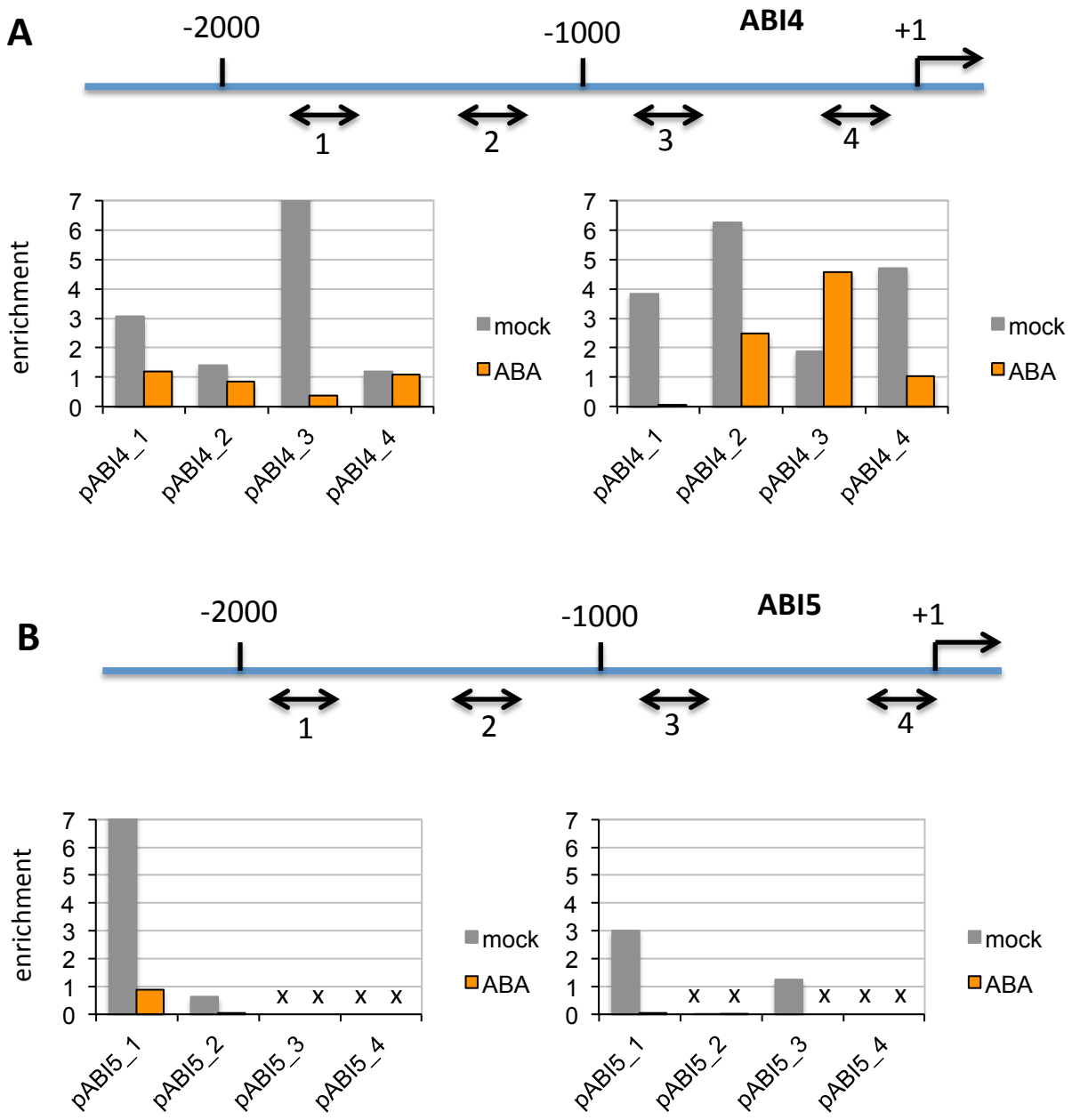


**Figure 6.** ChIP experiments made on ABI4 and ABI5 promoters. Chromatin IP was made with GFP-tagged ZFP3 overexpressing plants and promoter fragments of ABI4 and ABI5 genes were amplified by qPCR. Amplified fragments are indicated by double arrow (↔).

Results of two independent experiments are shown in the diagrams, which indicates the enrichment of the qPCR amplification. "x" indicates failed PCR reaction.

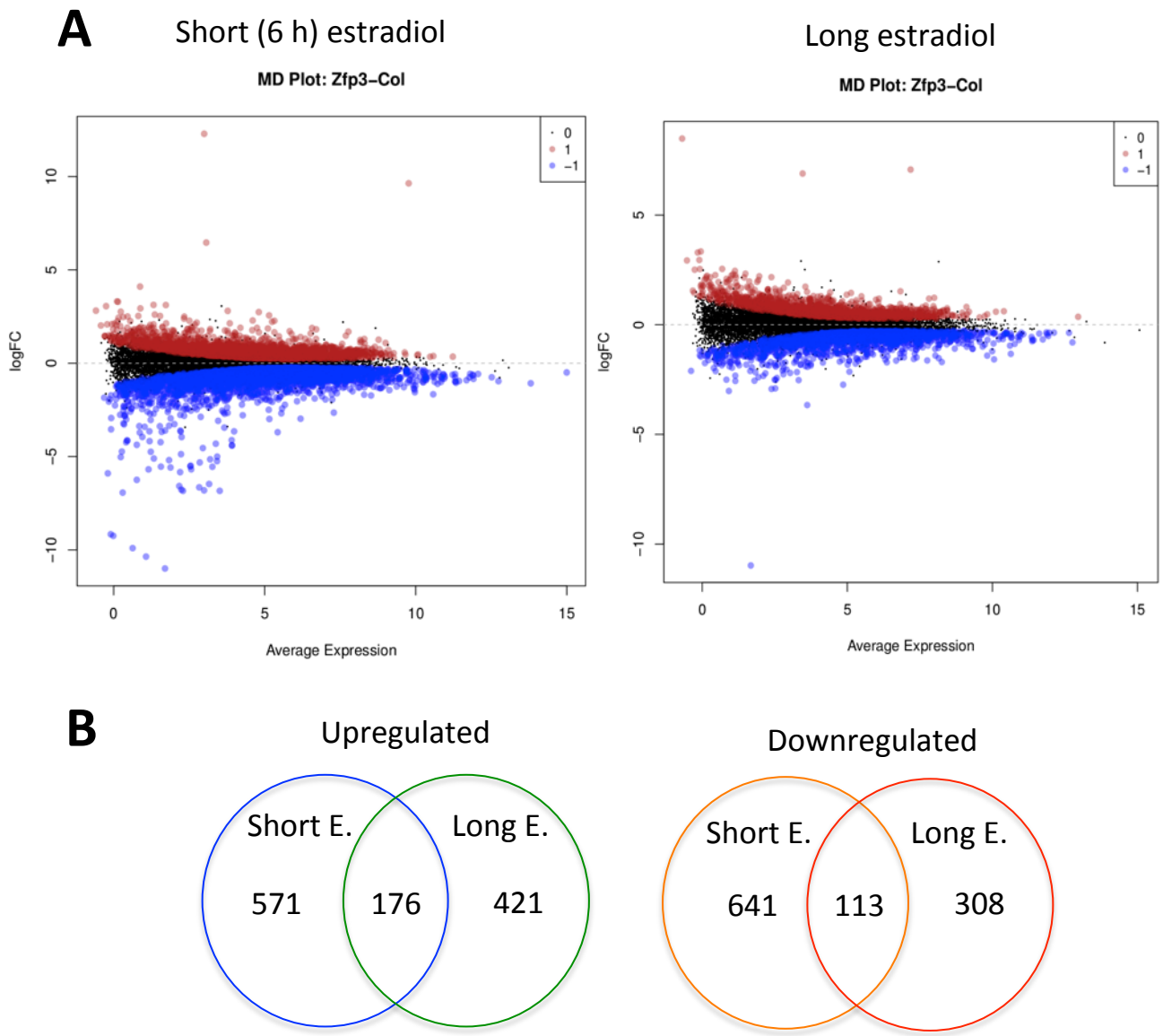


**Figure 7**. Summary of the transcript profiling experiment. A) MD plot of misregulated gene sets of short (6 h) and long estradiol-treated samples. Mean Difference plot indicates the log2(Fold Change) values versus mean logCPM expression values, highlighted genes have FDR<0.05. B) Number of up and downregulated genes (at least 2.5 fold change) in ZFP3 overexpressing plants. Short E. and Long E. indicates 6 h or continuous induction of XVE-ZFP3 by estradiol.

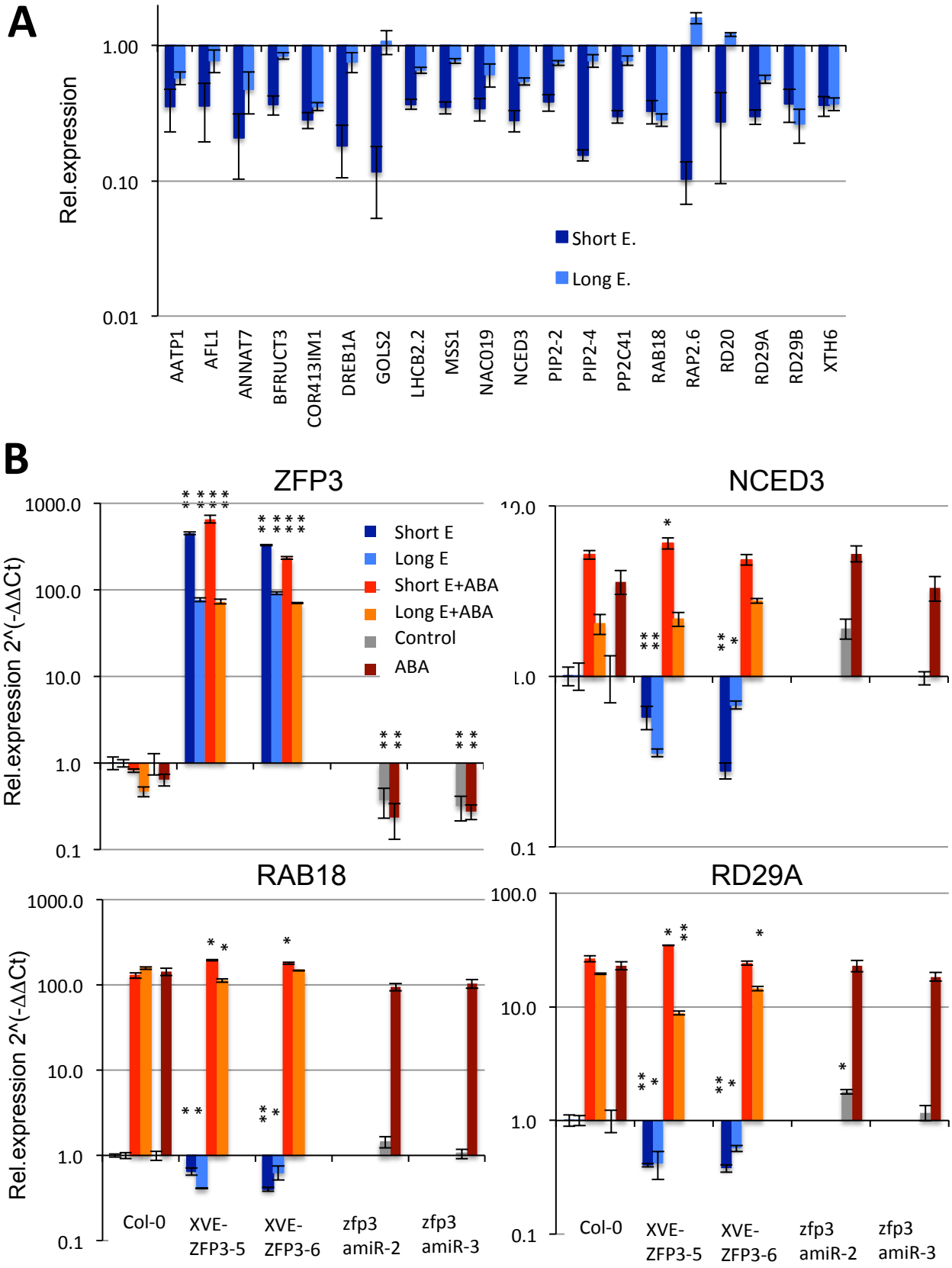


**Figure 8**. Expression of dehydration and ABA-induced genes in XVE-ZFP3 plants. A) Change in transcript levels of 20 genes. RNAseq data are shown in log scale, compared to transcript levels of Col-0 wild type plants (=1). B). Expression of ABA and dehydration induced *NCED3*, *RAB18* and *RD29A* genes in ZFP3 overexpressing (XVE-ZFP3) and silenced (zfp3amiR) plants.

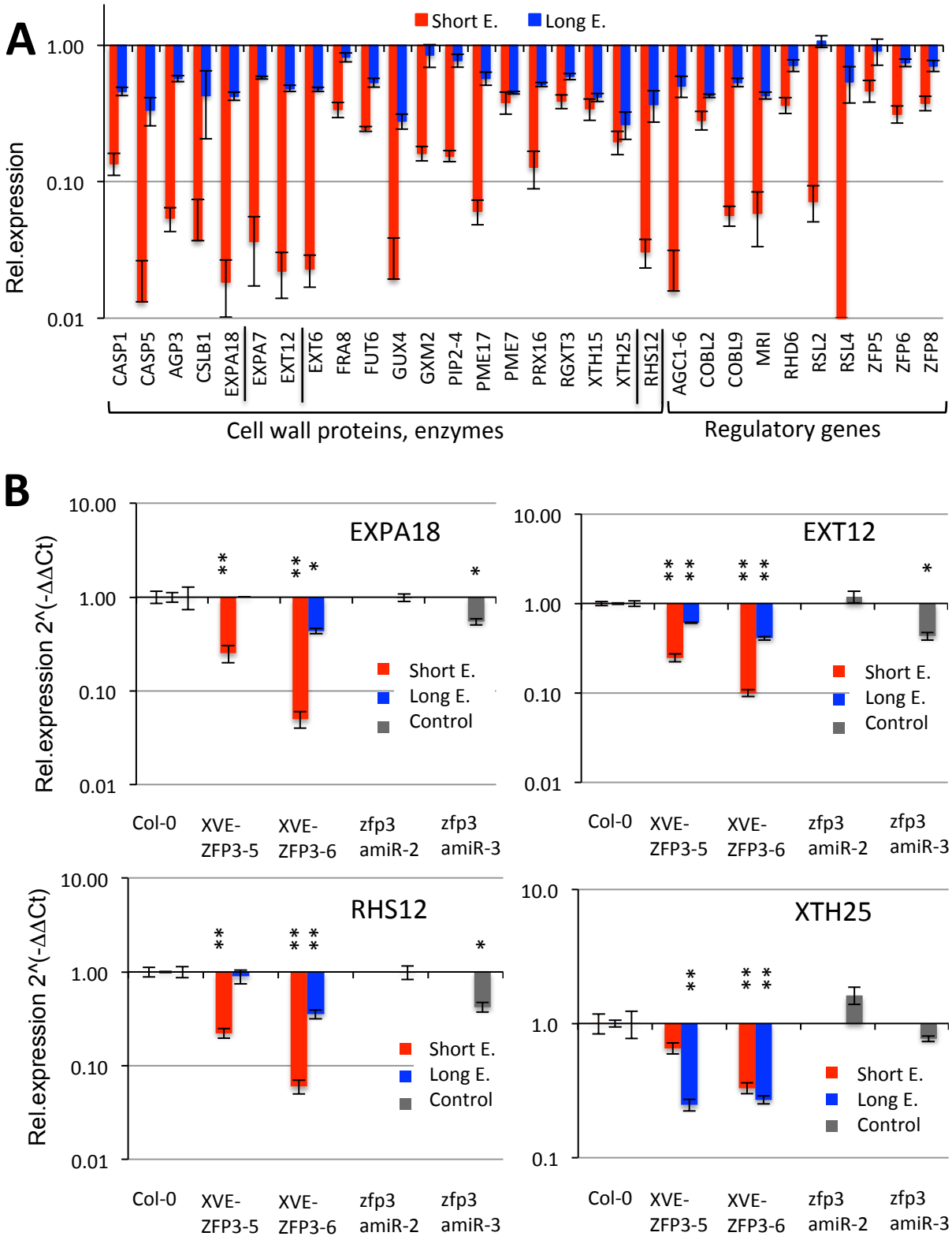


**Figure 9**. Expression of Arabidopsis genes implicated in cell wall formation, root hair growth and modification. A) Transcript levels of 30 cell wall and root hair-related genes obtained in RNA seq experiment. Relative transcript levels are show in log scale, compared to wild type plants (=1). B) qRT-PCR analysis of four cell wall and root hair-related genes: *EXPA18, EXT12, RHS12, XTH25*. Transcript levels were determined in two independent XVE-ZFP3 and zfp3amiR lines.

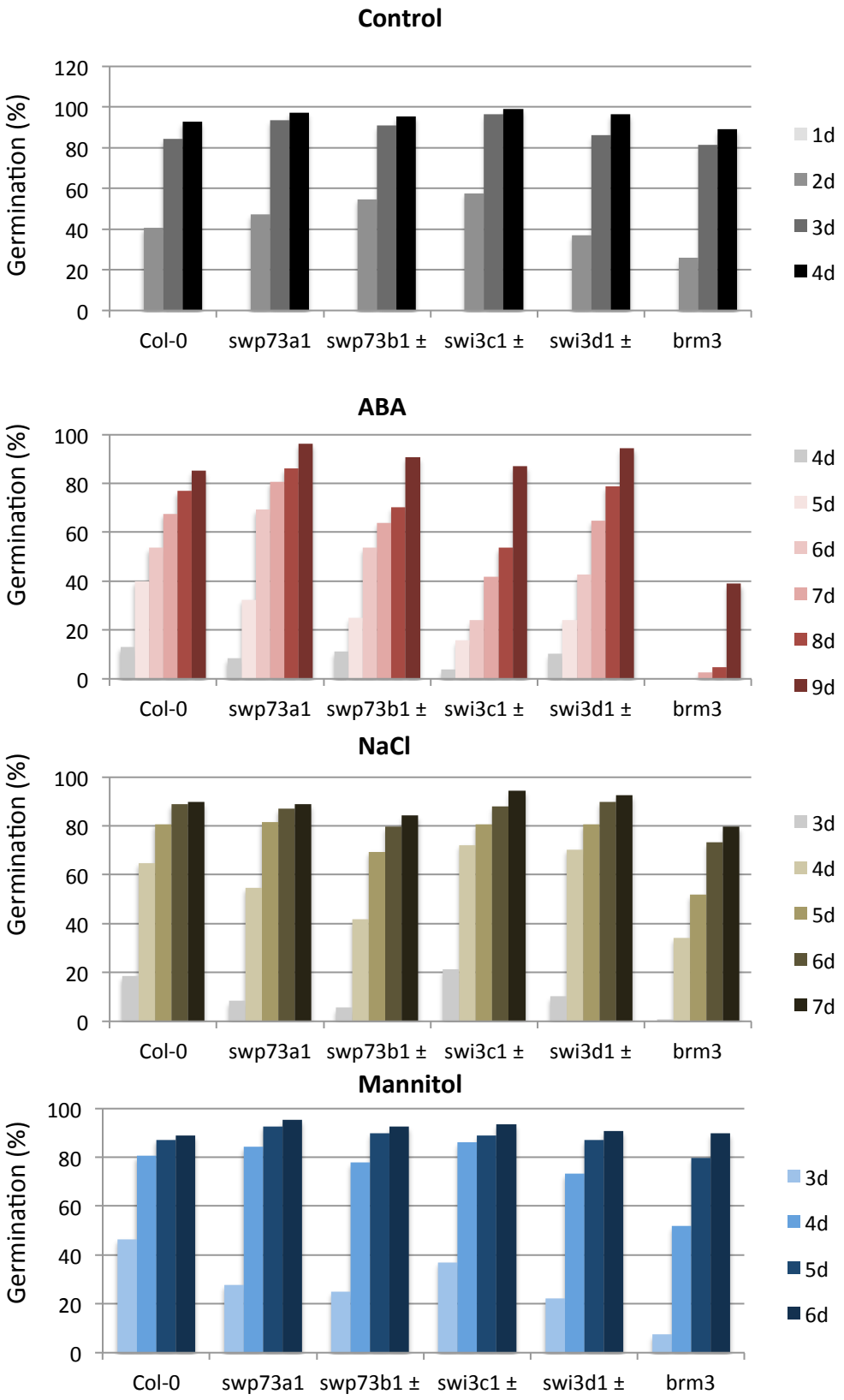


**Figure 10.** Germination of Col-0 wild type, and mutants of the SWI/SNF chromatin remodelling complex: swi73a1, swi73b1, swi3c1, swi3d1 and brm on media containing ABA (0.5 μM), NaCl (100 mM) and mannitol (200 mM). brm is hypersensitive to ABA, but other mutants had no difference to any additives.

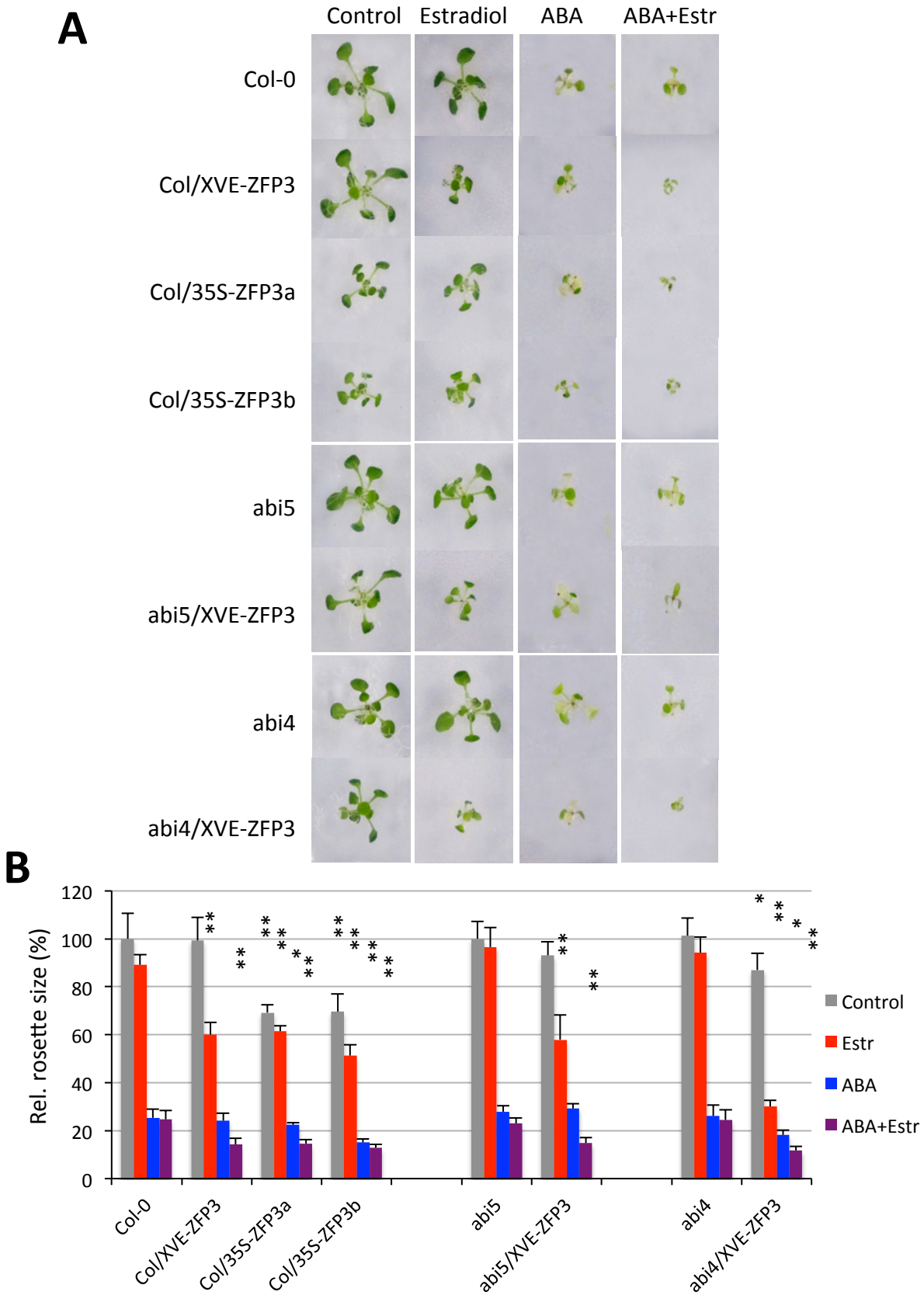


**Figure 11.** ABA sensitivity of in vitro-grown ZFP3 overexpressing plants. A) Typical rosettes of 14 days-old plants grown on media supplemented with 5 μM estradiol or 25 μM ABA or both for 9 days. Col-0: wild type, XVE-ZFP3: estradiol-inducible ZFP3, 35S-ZFP3a, Col/35S-ZFP3b: constitutively expressing, GFP or HA-tagged ZFP3. *abi5*, *abi4*: ABA insensitive 5 and ABA insensitive 4 mutants. B) Rosette sizes of 14 days-old plants Significant differences between rosette sizes of ZFP3 overexpressing and non expressing plants are shown by * ($p<0.05$) and ** ($p<0.01$) (N = 10) (Ttest).

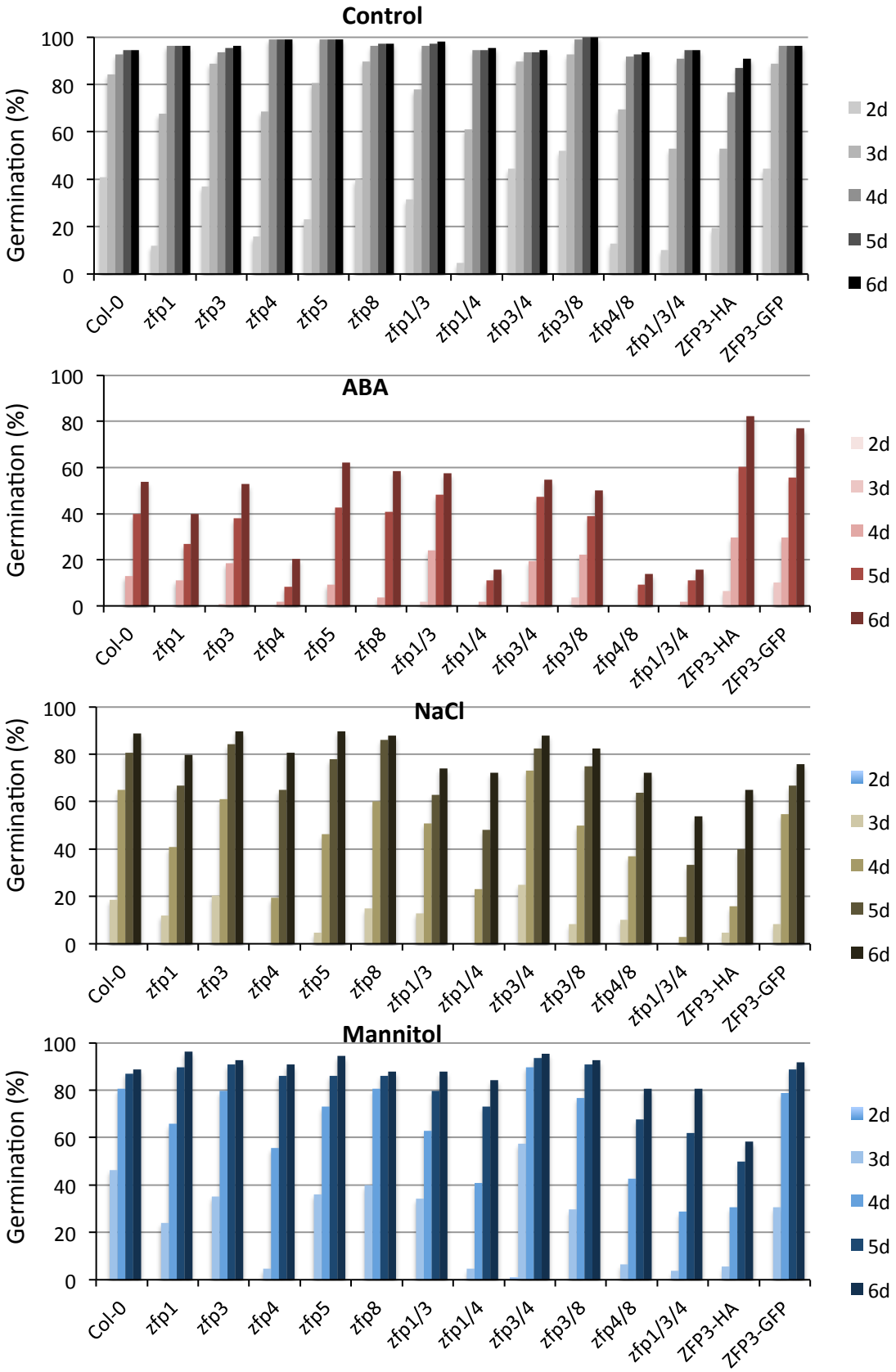


**Figure 12.** Germination of Col-0 wild type, single and crossed zfp mutants and ZFP3 overexpressing lines (35S-ZFP3-HA, 35S-ZFP3-GFP) on media supplemented by ABA (0.5 μM), NaCl (100 mM) and mannitol (200 mM). Note, that ABA represses germination of zfp4 mutant more than Col-0 wild type, while ZFP3-HA and ZFP3-GFP lines are insensitive. NaCl and mannitol reduces germination, but differences are not as big as with ABA.

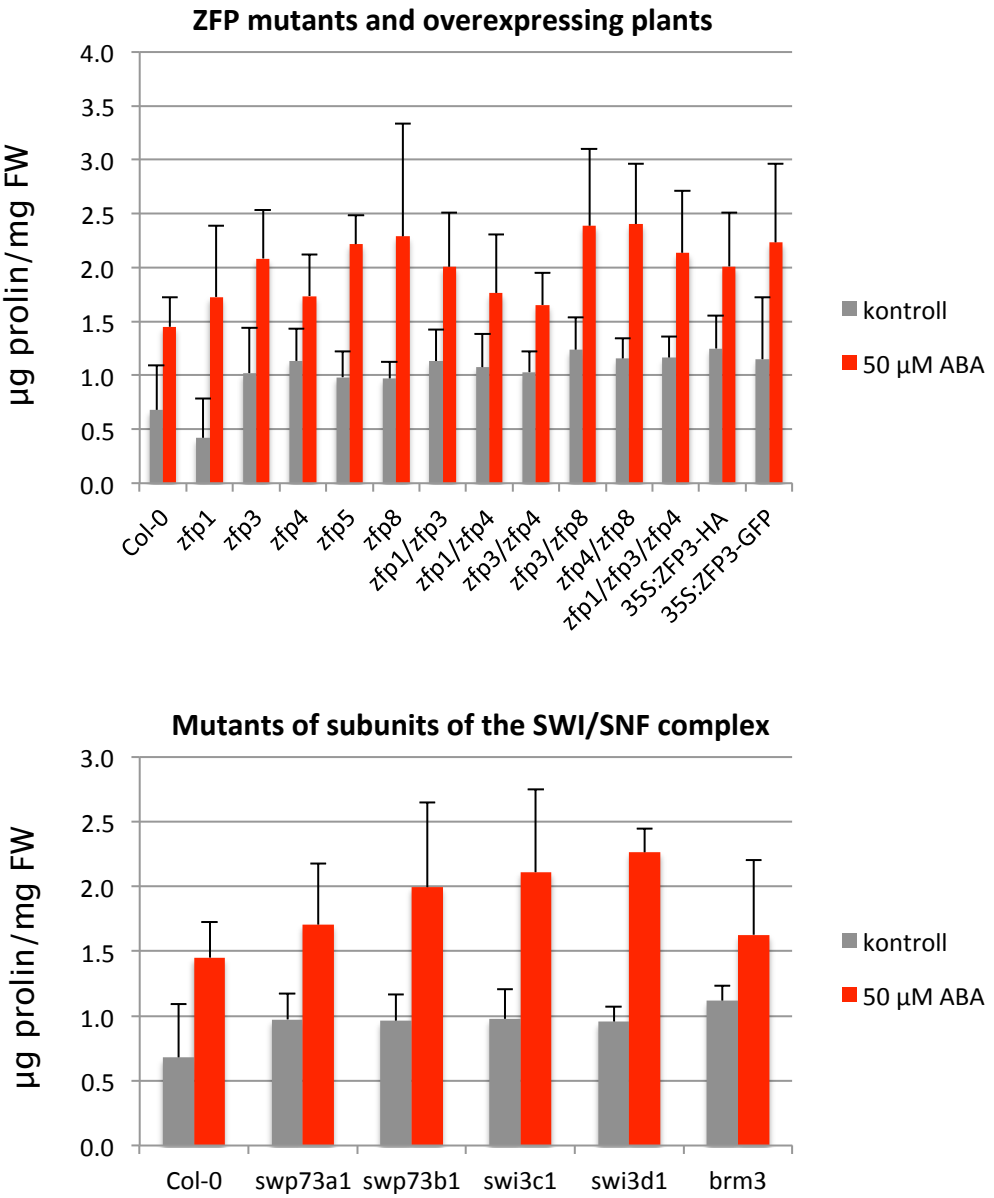


**Figure 13.** Proline accumulation in zfp single and crossed mutants, ZFP3 overexpressing plants and chromatin remodelling mutants.

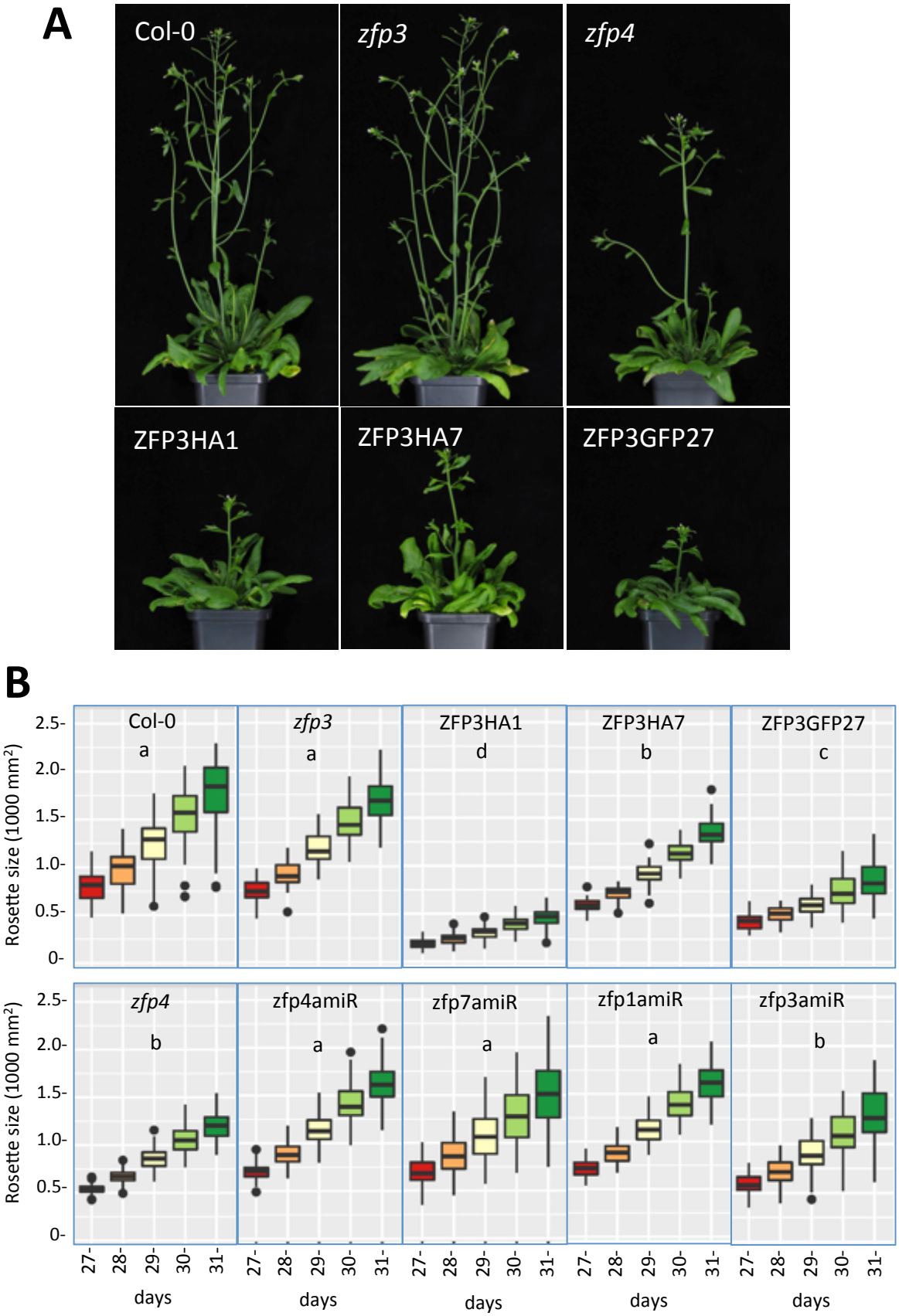


**Figure 14**. Plant phenotypes in greenhouse conditions. A) Images of a typical Col-0 plant, *zfp3* and *zfp4* mutants, and transgenic plants with 35S-ZFP3 gene constructs. B) Change in rosette areas of plants 27 to 31 days after germination. Different letters indicate significant differences between the genotypes (N=40, p-value < 0.05).

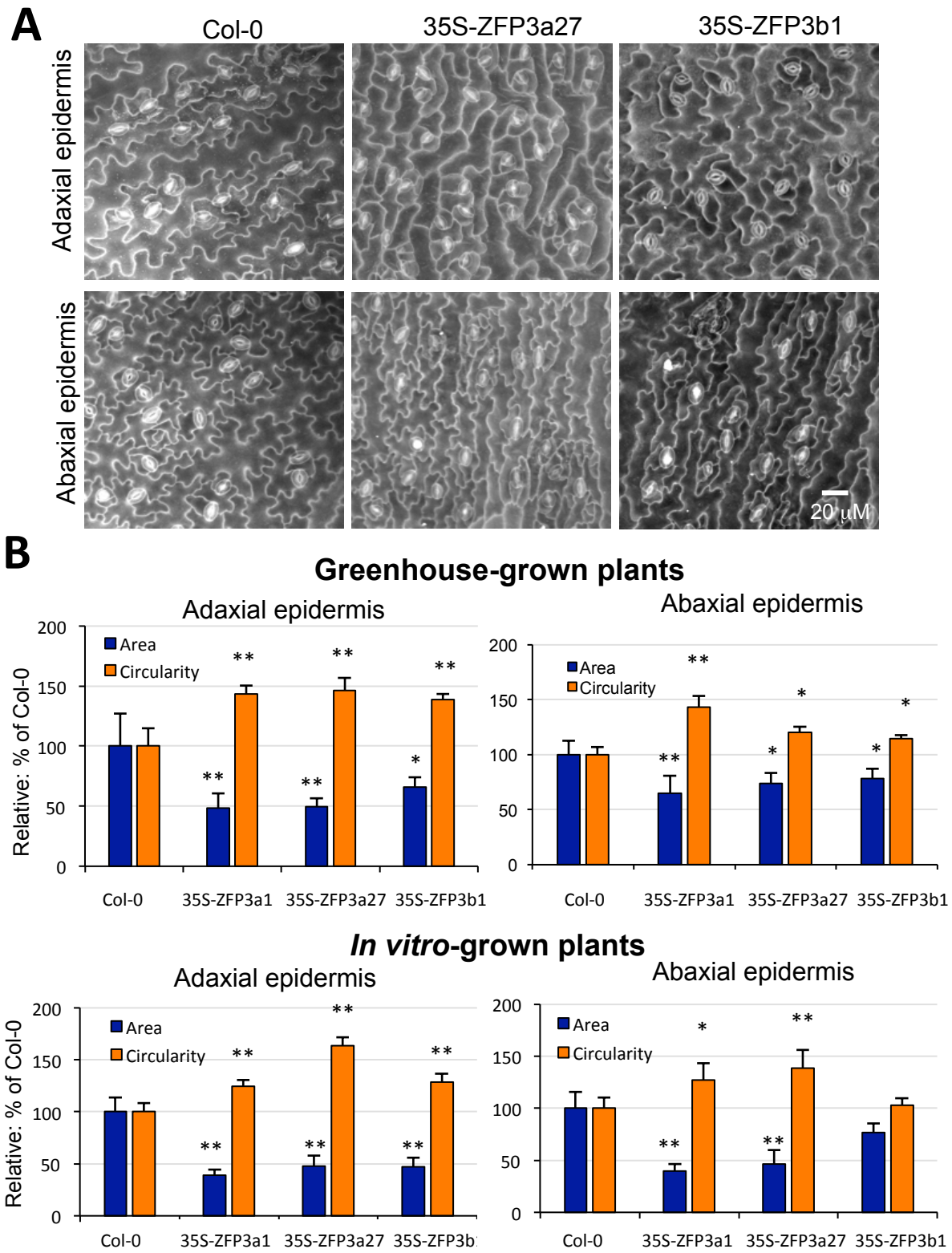


**Figure 15.** Leaf epidermal cells in scanning electron microscopic images. A) Typical images of leaf adaxial and abaxial surfaces of Col-0 and two 35S-ZFP3 plants. B) Quantitative analysis of epidermal cells. Average cell area and circularity are normalized to values obtained on wild type plants (=100%). Significant differences between Col-0 and transgenic plants are shown by * ($p<0.05$) and ** ($p<0.01$) (N = 40) (Ttest).

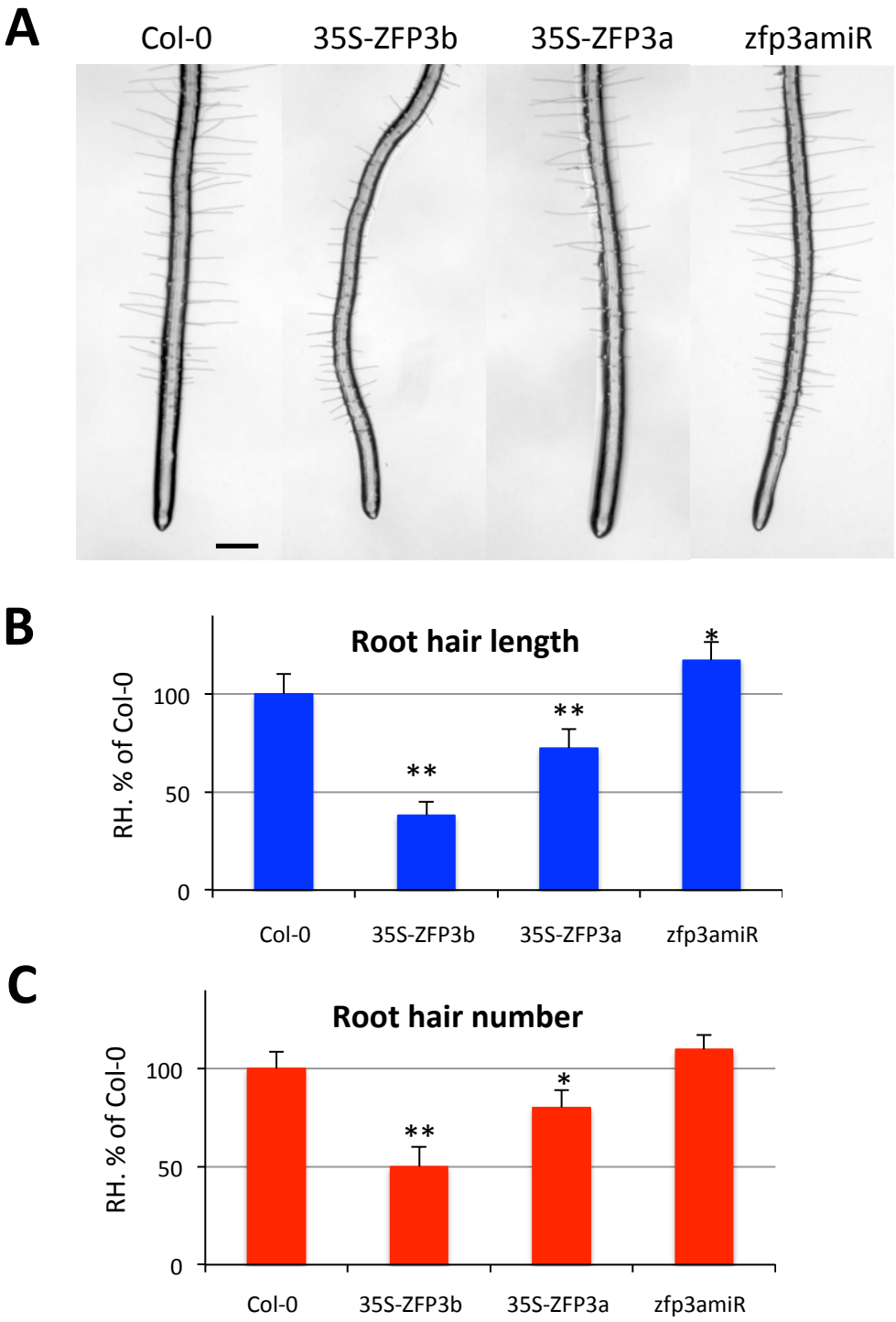


**Figure 16**. ZFP3 regulates root hair formation and elongation. A) Typical roots of in vitro-grown 35S-ZFP3 and zfp3amiR plants (scale bar = 200 mm). B,C) Average root hair lengths (b) and numbers (c) of ZFP3 overexpressing or silenced plants. Error bars on diagrams indicate standard error (No.=40), significant differences between root hair lengths of Col-0 and transgenic plants are shown by * ($p<0.05$) and ** ($p<0.01$) (Ttest).

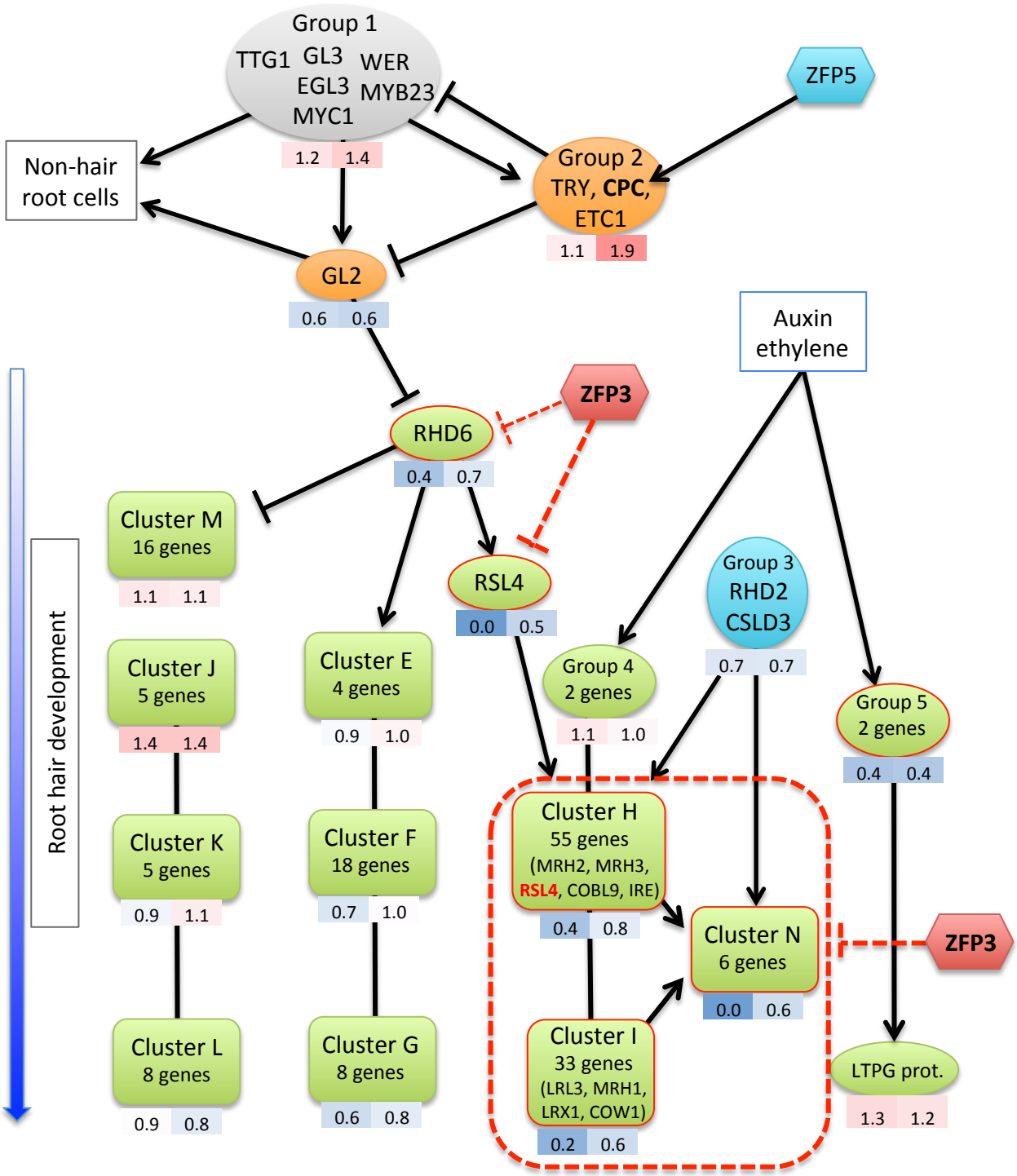


**Figure 17.** Model of root hair gene network, adapted from Bruex, et al., (2012). Transcriptional relationships of core root hair genes are shown, including the early transcription factor complex which determine fate of root hair and non-hair root cells (grey), the root hair specific genes (green), other regulatory genes (orange, blue) and ZFP3 (red). Averages of relative gene expression levels in ZFP3 overexpressing plants are shown under each symbol: left number indicates the effect of short (6 h), right number show the long (continuous) ZFP3 overexpression (red: induction, blue: repression). Clusters E-N corresponds to classification of Bruex, et al., (2012), groups 1-5 contain genes, which were not included into clusters.